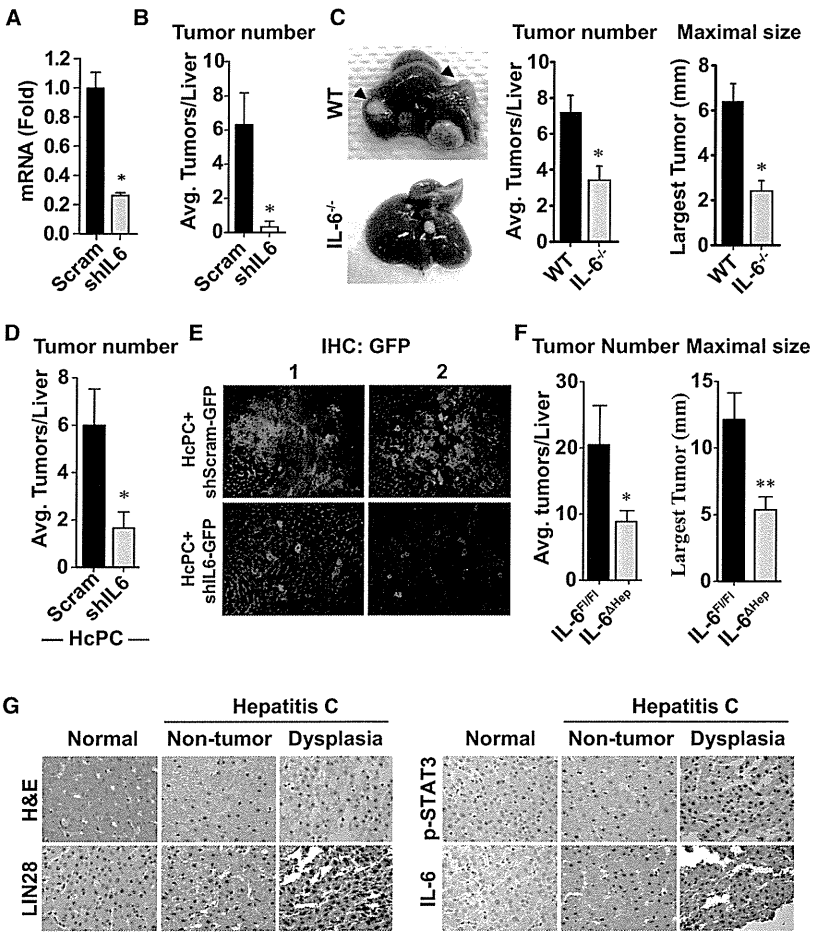

Figure 7. HCC Growth Depends on Autocrine IL-6 Production

(A) HCC cells (dih10) were transduced with lentiviruses containing scrambled or IL-6-specific shRNA. IL-6 mRNA was analyzed by qRT-PCR.

(B) Dih10 cells (1.2×10^5) transduced as above were i.s. injected into MUP-uPA mice that were analyzed 6 months later for HCC development (n = 3; ± SEM).

(C) HcPCs from WT and *Il6*$^{-/-}$ mice were injected (1×10^4 cells/mice) into MUP-uPA mice and analyzed 5 months later for HCC development (n = 5; ± SEM).

(D) HcPCs isolated from DEN-treated WT mice were transduced with shRNA against IL-6 or scrambled shRNA, cultured for 3 to 4 days, i.s. transplanted (1×10^4 cells/mice) into MUP-uPA mice, and analyzed 6 months later (n = 3; ± SEM).

(E) Livers of MUP-uPA mice from (D) were immunostained with GFP antibody 6 months after transplantation (200×). The bicistronic lentivirus in this experiment expresses GFP along with control or IL-6 shRNA, allowing tracking of the infected cells.

(F) DEN-treated *Il6*$^{\Delta hep}$ and *Il6*$^{F/F}$ mice were sacrificed after 9 months to evaluate tumor multiplicity and size (n = 6–10, ± SEM).

(G) IHC analysis of autocrine IL-6 signaling in human premalignant lesions in HCV-infected livers. Expression of LIN28, p-STAT3, and IL-6 was analyzed in 25 needle biopsies of dysplastic nodules, and representative positive specimens (n = 4) are shown. The dysplastic nodules and paired nontumor tissue were obtained from the same HCV-infected patient (n = 25). Nontumor tissue of metastatic liver cancer was used as normal control.

See also Figures S6 and S7.

(Duncan et al., 2009). Notably, GO analysis revealed that many of the genes whose expression is downregulated in HcPC-containing aggregates are involved in xenobiotic and organic acid metabolism, characteristics of differentiated hepatocytes. The same types of genes are also downregulated in HCC. However, final identification of the origin of HcPC will be provided by ongoing lineage-tracing experiments.

The Significance of Autocrine IL-6 Expression

Elevated IL-6 was detected in at least 40% of human HCCs, where it is expressed by the cancer cells (Soresi et al., 2006). More recent studies have confirmed upregulation of IL-6 in human HCC and suggested that it plays a central role in a gene expression network that drives tumor development (Ji et al., 2009). Elevated IL-6 was also found in viral and alcoholic hepatitis and liver cirrhosis, but in these conditions, IL-6 is expressed mainly by myeloid cells/leukocytes rather than parenchymal cells (Deviere et al., 1989; Kakumu et al., 1993; Soresi et al., 2006). Our studies indicate that the critical site of IL-6 expression shifts from myeloid cells to epithelial cells during the course of DEN-induced liver tumorigenesis. Initially, DEN administration rapidly induces IL-6 in Kupffer cells through NF-κB activation (Maeda et al., 2005). This initial surge in IL-6 is required for DEN-induced hepatocarcinogenesis (Naugler et al., 2007). Although IL-6 decays within 2 weeks of DEN administration, it reappears several months later, but at that time, it is expressed within FAH. IL-6 expression is also elevated in isolated HcPCs and is maintained in fully transformed HCC cells. Furthermore, autocrine IL-6 is important for HcPC to HCC progression and for tumorigenic growth. Autocrine IL-6 in both HcPC and HCC cells depends on elevated expression of LIN28, an RNA-binding protein that exerts its protumorigenic activity through downregulation of Let-7, an miRNA that inhibits IL-6 expression (Viswanathan and Daley, 2010). Accordingly, HcPCs exhibit downregulation of both Let-7f and Let-7g, and elevated LIN28 is found not only in isolated HcPCs but also within FAH and human HCV-induced dysplastic lesions.

A similar LIN28-Let-7-IL-6 epigenetic switch is important for in vitro programming and maintenance of cancer stem cells (Iliopoulos et al., 2009). IL-6 also induces malignant features in human ductal carcinoma stem cells (Sansone et al., 2007). In fact, autocrine IL-6 signaling was suggested to play a key role in STAT3-dependent tumor progression (Grivennikov and Karin, 2008). Another miRNA-driven autoregulatory circuit involved in

hepatocarcinogenesis accounts for elevated IL-6R expression (Hatziapostolou et al., 2011). Yet, HcPC-containing aggregates also express several other STAT3-activiting cytokines and receptors. Accordingly, silencing or ablation of IL-6 results in incomplete inhibition of HcPC to HCC progression. Nonetheless, our results demonstrate that autoregulatory circuits/epigenetic switches play an important role in the very early stages of tumorigenesis. Given that such circuits are already activated in premalignant cells, pharmacological agents that disrupt their function may be useful in cancer prevention. Prevention is of particular importance in cancers such as HCC, which is often detected at a stage that is refractory to currently available therapeutics.

EXPERIMENTAL PROCEDURES

Mice, HCC Induction, HcPC Isolation, and Transplantation

MUP-uPA transgenic mice (Weglarz et al., 2000) were maintained on a pure BL/6 background. Because homozygous females frequently die when pregnant, MUP-uPA heterozygotes were generated by backcrossing homozygous MUP-uPA males with BL/6 females to be used as recipients for hepatic transplantation. *Tak1*$^{\Delta hep}$ (Inokuchi et al., 2010) and *Il6*$^{F/F}$ (Quintana et al., 2013) mice were also in the BL/6 background. *Il6*$^{\Delta hep}$ mice were generated by crossing *Il6*$^{F/F}$ and *Alb-Cre* mice. C57BL/6 actin-GFP mice were from the Jackson Laboratories. BL/6 mice were purchased from Charles River Laboratories.

To induce HCC, 15-day-old mice were injected i.p. with 25 mg/kg DEN (Sigma). A pool of DEN-injected BL/6 mice was maintained and used in most experiments. Hepatocytes were isolated using a two-step procedure (He et al., 2010). Cell aggregates were isolated by filtration through 70 and 40 μm sieves. To disperse the aggregates into single cells, they were subjected to gentle pipetting in Ca/Mg-free PBS on ice. Single-cell suspensions of aggregated and nonaggregated hepatocytes were transplanted via an i.s. injection into 21-day-old male MUP-uPA mice (He et al., 2010). Alternatively, single-cell suspensions of aggregated hepatocytes were enriched for CD44^{+} HcPC using magnetic beads. As few as 100 viable CD44^{+} cells mixed with 1×10^{5} normal hepatocytes from normal males were transplanted into MUP-uPA mice. Alternatively, BL/6 mice were pretreated with retrorsine (70 mg/kg i.p.) (Sigma), a cell-cycle inhibitor, 1 month prior to transplantation. Transplanted mice were allowed to recover for 1 week and then injected weekly with 3× 0.5 ml/kg CCl_4 i.p. to induce liver injury and hepatocyte proliferation (Guo et al., 2002). Mice were sacrificed 5 to 6 months later, and tumors bigger than 1 mm in diameter on the liver surface were counted. Tumors bigger than 5 mm across were dissected for biochemical and molecular analyses.

ACCESSION NUMBERS

Raw gene expression array data have been deposited to NCBI's Gene Expression Omnibus under the GSE50431 study.

SUPPLEMENTAL INFORMATION

Supplemental Information includes Extended Experimental Procedures, seven figures, and three tables and can be found with this article online at http://dx.doi.org/10.1016/j.cell.2013.09.031.

AUTHOR CONTRIBUTIONS

G.H. identified, isolated, and characterized HcPCs; D.D. and H.N. optimized the HcPC isolation and purification procedure; D.D. found the mechanism of their dependence on autocrine IL-6 controlled by LIN28, characterized them using flow cytometry (with S.S.), and conducted miR analyses (with M.H. and D.I.); H.N. and D.D. used *Il6*$^{\Delta hep}$ mice to demonstrate in vivo HCC dependency on autocrine IL-6; H.N. (with R.T. and K.K.) found IL-6, LIN28, and P-STAT3 in human dysplastic lesions; J.F.-B. conducted the transcriptome analysis and exome sequencing (with S.E.Y., K.J., and O.H.) and with H.O. examined oncogenic potential of oval cells; H.O. examined HcPC proliferative potential and performed IF analysis of isolated HcPC (with A.S. and R.M.H.); Y.J. assisted with IHC and ISH staining; E.S. contributed to the experiments involving *Tak1*$^{\Delta hep}$ mice; G.H., D.D., J.F.-B., H.O., and M.K. wrote the manuscript.

ACKNOWLEDGMENTS

We acknowledge the Biogem facility at UCSD for their assistance with transcriptome analysis and A. Arian, K. Iwaisako, Y. Hiroshima, and H. Matsui for technical assistance. We thank Dr. J. Hidalgo (Universitat Autonoma de Barcelona, Spain) for the *Il6*$^{F/F}$ mice. Research was supported by the Superfund Basic Research Program (P42ES010337), NIH (CA118165 and CA155120), Wellcome Trust (WT086755), American Diabetes Association (7-08-MN-29), the Center for Translational Science (UL1RR031980 and UL1TR000100), the National Center for Research Resources IMAT program (N12R1CA155615), and postdoctoral research fellowships from the Damon Runyon Cancer Research Foundation (G.H.), American Liver Foundation (D.D.), Daiichi Sankyo Foundation of Life Science (H.N.), California Institute for Regenerative Medicine Stem Cell Training Grant II (TG2-01154) fellowship (J.F.-B.), Kanzawa Medical Research Foundation (H.O.), the German Research Foundation (DFG, SH721/1-1 to S.S.), and a Young Investigator Award from the National Childhood Cancer Foundation, "CureSearch" (D.D.). M.K. is an ACS Research Professor and is a recipient of the Ben and Wanda Hildyard Chair for Mitochondrial and Metabolic Diseases.

Received: December 11, 2012
Revised: June 4, 2013
Accepted: September 19, 2013
Published: October 10, 2013

REFERENCES

Bannasch, P. (1984). Sequential cellular changes during chemical carcinogenesis. J. Cancer Res. Clin. Oncol. *108*, 11–22.

Bladt, F., Riethmacher, D., Isenmann, S., Aguzzi, A., and Birchmeier, C. (1995). Essential role for the c-met receptor in the migration of myogenic precursor cells into the limb bud. Nature *376*, 768–771.

Deviere, J., Content, J., Denys, C., Vandenbussche, P., Schandene, L., Wybran, J., and Dupont, E. (1989). High interleukin-6 serum levels and increased production by leucocytes in alcoholic liver cirrhosis. Correlation with IgA serum levels and lymphokines production. Clin. Exp. Immunol. *77*, 221–225.

Dorrell, C., Erker, L., Schug, J., Kopp, J.L., Canaday, P.S., Fox, A.J., Smirnova, O., Duncan, A.W., Finegold, M.J., Sander, M., et al. (2011). Prospective isolation of a bipotential clonogenic liver progenitor cell in adult mice. Genes Dev. *25*, 1193–1203.

Duncan, A.W., Dorrell, C., and Grompe, M. (2009). Stem cells and liver regeneration. Gastroenterology *137*, 466–481.

Eferl, R., Ricci, R., Kenner, L., Zenz, R., David, J.P., Rath, M., and Wagner, E.F. (2003). Liver tumor development. c-Jun antagonizes the proapoptotic activity of p53. Cell *112*, 181–192.

El-Serag, H.B. (2011). Hepatocellular carcinoma. N. Engl. J. Med. *365*, 1118–1127.

Grivennikov, S., and Karin, M. (2008). Autocrine IL-6 signaling: a key event in tumorigenesis? Cancer Cell *13*, 7–9.

Guichard, C., Amaddeo, G., Imbeaud, S., Ladeiro, Y., Pelletier, L., Maad, I.B., Calderaro, J., Bioulac-Sage, P., Letexier, M., Degos, F., et al. (2012). Integrated analysis of somatic mutations and focal copy-number changes identifies key genes and pathways in hepatocellular carcinoma. Nat. Genet. *44*, 694–698.

Guo, D., Fu, T., Nelson, J.A., Superina, R.A., and Soriano, H.E. (2002). Liver repopulation after cell transplantation in mice treated with retrorsine and carbon tetrachloride. Transplantation *73*, 1818–1824.

Guo, X., Xiong, L., Sun, T., Peng, R., Zou, L., Zhu, H., Zhang, J., Li, H., and Zhao, J. (2012). Expression features of SOX9 associate with tumor progression and poor prognosis of hepatocellular carcinoma. Diagn. Pathol. *7*, 44.

Haridass, D., Yuan, Q., Becker, P.D., Cantz, T., Iken, M., Rothe, M., Narain, N., Bock, M., Nörder, M., Legrand, N., et al. (2009). Repopulation efficiencies of adult hepatocytes, fetal liver progenitor cells, and embryonic stem cell-derived hepatic cells in albumin-promoter-enhancer urokinase-type plasminogen activator mice. Am. J. Pathol. *175*, 1483–1492.

Hatziapostolou, M., Polytarchou, C., Aggelidou, E., Drakaki, A., Poultsides, G.A., Jaeger, S.A., Ogata, H., Karin, M., Struhl, K., Hadzopoulou-Cladaras, M., and Iliopoulos, D. (2011). An HNF4α-miRNA inflammatory feedback circuit regulates hepatocellular oncogenesis. Cell *147*, 1233–1247.

He, G., Yu, G.Y., Temkin, V., Ogata, H., Kuntzen, C., Sakurai, T., Sieghart, W., Peck-Radosavljevic, M., Leffert, H.L., and Karin, M. (2010). Hepatocyte IKKbeta/NF-kappaB inhibits tumor promotion and progression by preventing oxidative stress-driven STAT3 activation. Cancer Cell *17*, 286–297.

Hruban, R.H., Maitra, A., Kern, S.E., and Goggins, M. (2007). Precursors to pancreatic cancer. Gastroenterol. Clin. North Am. *36*, 831–849, vi.

Hytiroglou, P., Park, Y.N., Krinsky, G., and Theise, N.D. (2007). Hepatic precancerous lesions and small hepatocellular carcinoma. Gastroenterol. Clin. North Am. *36*, 867–887, vii.

Ichinohe, N., Kon, J., Sasaki, K., Nakamura, Y., Ooe, H., Tanimizu, N., and Mitaka, T. (2012). Growth ability and repopulation efficiency of transplanted hepatic stem cells, progenitor cells, and mature hepatocytes in retrorsine-treated rat livers. Cell Transplant. *21*, 11–22.

Iliopoulos, D., Hirsch, H.A., and Struhl, K. (2009). An epigenetic switch involving NF-kappaB, Lin28, Let-7 MicroRNA, and IL6 links inflammation to cell transformation. Cell *139*, 693–706.

Inokuchi, S., Aoyama, T., Miura, K., Osterreicher, C.H., Kodama, Y., Miyai, K., Akira, S., Brenner, D.A., and Seki, E. (2010). Disruption of TAK1 in hepatocytes causes hepatic injury, inflammation, fibrosis, and carcinogenesis. Proc. Natl. Acad. Sci. USA *107*, 844–849.

Ji, J., Shi, J., Budhu, A., Yu, Z., Forgues, M., Roessler, S., Ambs, S., Chen, Y., Meltzer, P.S., Croce, C.M., et al. (2009). MicroRNA expression, survival, and response to interferon in liver cancer. N. Engl. J. Med. *361*, 1437–1447.

Kakumu, S., Shinagawa, T., Ishikawa, T., Yoshioka, K., Wakita, T., and Ida, N. (1993). Interleukin 6 production by peripheral blood mononuclear cells in patients with chronic hepatitis B virus infection and primary biliary cirrhosis. Gastroenterol. Jpn. *28*, 18–24.

Kang, J.S., Wanibuchi, H., Morimura, K., Gonzalez, F.J., and Fukushima, S. (2007). Role of CYP2E1 in diethylnitrosamine-induced hepatocarcinogenesis in vivo. Cancer Res. *67*, 11141–11146.

Laconi, E., Oren, R., Mukhopadhyay, D.K., Hurston, E., Laconi, S., Pani, P., Dabeva, M.D., and Shafritz, D.A. (1998). Long-term, near-total liver replacement by transplantation of isolated hepatocytes in rats treated with retrorsine. Am. J. Pathol. *153*, 319–329.

Maeda, S., Kamata, H., Luo, J.L., Leffert, H., and Karin, M. (2005). IKKbeta couples hepatocyte death to cytokine-driven compensatory proliferation that promotes chemical hepatocarcinogenesis. Cell *121*, 977–990.

Marquardt, J.U., and Thorgeirsson, S.S. (2010). Stem cells in hepatocarcinogenesis: evidence from genomic data. Semin. Liver Dis. *30*, 26–34.

Meyer, K., Lee, J.S., Dyck, P.A., Cao, W.Q., Rao, M.S., Thorgeirsson, S.S., and Reddy, J.K. (2003). Molecular profiling of hepatocellular carcinomas developing spontaneously in acyl-CoA oxidase deficient mice: comparison with liver tumors induced in wild-type mice by a peroxisome proliferator and a genotoxic carcinogen. Carcinogenesis *24*, 975–984.

Mikhail, S., and He, A.R. (2011). Liver cancer stem cells. Int. J. Hepatol. *2011*, 486954.

Naugler, W.E., Sakurai, T., Kim, S., Maeda, S., Kim, K., Elsharkawy, A.M., and Karin, M. (2007). Gender disparity in liver cancer due to sex differences in MyD88-dependent IL-6 production. Science *317*, 121–124.

Nguyen, L.V., Vanner, R., Dirks, P., and Eaves, C.J. (2012). Cancer stem cells: an evolving concept. Nat. Rev. Cancer *12*, 133–143.

Nowell, P.C. (1976). The clonal evolution of tumor cell populations. Science *194*, 23–28.

Park, E.J., Lee, J.H., Yu, G.Y., He, G., Ali, S.R., Holzer, R.G., Osterreicher, C.H., Takahashi, H., and Karin, M. (2010). Dietary and genetic obesity promote liver inflammation and tumorigenesis by enhancing IL-6 and TNF expression. Cell *140*, 197–208.

Pitot, H.C. (1990). Altered hepatic foci: their role in murine hepatocarcinogenesis. Annu. Rev. Pharmacol. Toxicol. *30*, 465–500.

Porta, C., De Amici, M., Quaglini, S., Paglino, C., Tagliani, F., Boncimino, A., Moratti, R., and Corazza, G.R. (2008). Circulating interleukin-6 as a tumor marker for hepatocellular carcinoma. Ann. Oncol. *19*, 353–358.

Quintana, A., Erta, M., Ferrer, B., Comes, G., Giralt, M., and Hidalgo, J. (2013). Astrocyte-specific deficiency of interleukin-6 and its receptor reveal specific roles in survival, body weight and behavior. Brain Behav. Immun. *27*, 162–173.

Rabes, H.M. (1983). Development and growth of early preneoplastic lesions induced in the liver by chemical carcinogens. J. Cancer Res. Clin. Oncol. *106*, 85–92.

Rhim, J.A., Sandgren, E.P., Degen, J.L., Palmiter, R.D., and Brinster, R.L. (1994). Replacement of diseased mouse liver by hepatic cell transplantation. Science *263*, 1149–1152.

Sansone, P., Storci, G., Tavolari, S., Guarnieri, T., Giovannini, C., Taffurelli, M., Ceccarelli, C., Santini, D., Paterini, P., Marcu, K.B., et al. (2007). IL-6 triggers malignant features in mammospheres from human ductal breast carcinoma and normal mammary gland. J. Clin. Invest. *117*, 3988–4002.

Seki, S., Sakaguchi, H., Kitada, T., Tamori, A., Takeda, T., Kawada, N., Habu, D., Nakatani, K., Nishiguchi, S., and Shiomi, S. (2000). Outcomes of dysplastic nodules in human cirrhotic liver: a clinicopathological study. Clin. Cancer Res. *6*, 3469–3473.

Sell, S., and Leffert, H.L. (2008). Liver cancer stem cells. J. Clin. Oncol. *26*, 2800–2805.

Shin, S., Walton, G., Aoki, R., Brondell, K., Schug, J., Fox, A., Smirnova, O., Dorrell, C., Erker, L., Chu, A.S., et al. (2011). Foxl1-Cre-marked adult hepatic progenitors have clonogenic and bilineage differentiation potential. Genes Dev. *25*, 1185–1192.

Soresi, M., Giannitrapani, L., D'Antona, F., Florena, A.M., La Spada, E., Terranova, A., Cervello, M., D'Alessandro, N., and Montalto, G. (2006). Interleukin-6 and its soluble receptor in patients with liver cirrhosis and hepatocellular carcinoma. World J. Gastroenterol. *12*, 2563–2568.

Su, Y., Kanamoto, R., Miller, D.A., Ogawa, H., and Pitot, H.C. (1990). Regulation of the expression of the serine dehydratase gene in the kidney and liver of the rat. Biochem. Biophys. Res. Commun. *170*, 892–899.

Su, Q., Benner, A., Hofmann, W.J., Otto, G., Pichlmayr, R., and Bannasch, P. (1997). Human hepatic preneoplasia: phenotypes and proliferation kinetics of foci and nodules of altered hepatocytes and their relationship to liver cell dysplasia. Virchows Arch. *431*, 391–406.

Takayama, T., Makuuchi, M., Hirohashi, S., Sakamoto, M., Okazaki, N., Takayasu, K., Kosuge, T., Motoo, Y., Yamazaki, S., and Hasegawa, H. (1990). Malignant transformation of adenomatous hyperplasia to hepatocellular carcinoma. Lancet *336*, 1150–1153.

Terris, B., Cavard, C., and Perret, C. (2010). EpCAM, a new marker for cancer stem cells in hepatocellular carcinoma. J. Hepatol. *52*, 280–281.

Tsutsumi, M., Lasker, J.M., Shimizu, M., Rosman, A.S., and Lieber, C.S. (1989). The intralobular distribution of ethanol-inducible P450IIE1 in rat and human liver. Hepatology *10*, 437–446.

Verna, L., Whysner, J., and Williams, G.M. (1996). N-nitrosodiethylamine mechanistic data and risk assessment: bioactivation, DNA-adduct formation, mutagenicity, and tumor initiation. Pharmacol. Ther. *71*, 57–81.

Viswanathan, S.R., and Daley, G.Q. (2010). Lin28: A microRNA regulator with a macro role. Cell *140*, 445–449.

Wang, R., Ferrell, L.D., Faouzi, S., Maher, J.J., and Bishop, J.M. (2001). Activation of the Met receptor by cell attachment induces and sustains hepatocellular carcinomas in transgenic mice. J. Cell Biol. *153*, 1023–1034.

Weglarz, T.C., Degen, J.L., and Sandgren, E.P. (2000). Hepatocyte transplantation into diseased mouse liver. Kinetics of parenchymal repopulation and identification of the proliferative capacity of tetraploid and octaploid hepatocytes. Am. J. Pathol. *157*, 1963–1974.

Wood, L.D., Parsons, D.W., Jones, S., Lin, J., Sjöblom, T., Leary, R.J., Shen, D., Boca, S.M., Barber, T., Ptak, J., et al. (2007). The genomic landscapes of human breast and colorectal cancers. Science *318*, 1108–1113.

Yamashita, T., Forgues, M., Wang, W., Kim, J.W., Ye, Q., Jia, H., Budhu, A., Zanetti, K.A., Chen, Y., Qin, L.X., et al. (2008). EpCAM and alpha-fetoprotein expression defines novel prognostic subtypes of hepatocellular carcinoma. Cancer Res. *68*, 1451–1461.

Yang, Z.F., Ho, D.W., Ng, M.N., Lau, C.K., Yu, W.C., Ngai, P., Chu, P.W., Lam, C.T., Poon, R.T., and Fan, S.T. (2008). Significance of CD90+ cancer stem cells in human liver cancer. Cancer Cell *13*, 153–166.

Zheng, T., Wang, J., Jiang, H., and Liu, L. (2011). Hippo signaling in oval cells and hepatocarcinogenesis. Cancer Lett. *28*, 91–99.

Zhu, Z., Hao, X., Yan, M., Yao, M., Ge, C., Gu, J., and Li, J. (2010). Cancer stem/progenitor cells are highly enriched in CD133+CD44+ population in hepatocellular carcinoma. Int. J. Cancer *126*, 2067–2078.

Zöller, M. (2009). Tetraspanins: push and pull in suppressing and promoting metastasis. Nat. Rev. Cancer *9*, 40–55.

SCIENTIFIC REPORTS

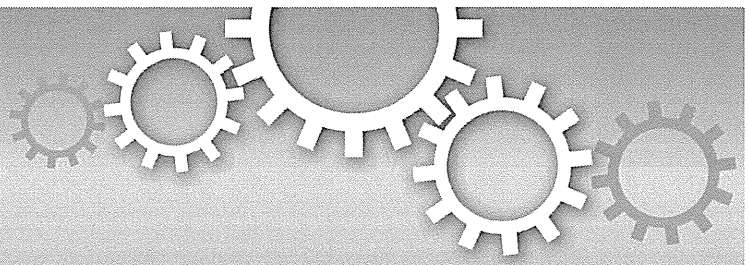

OPEN

SUBJECT AREAS:
TUMOUR IMMUNOLOGY
CANCER PREVENTION
LIVER CANCER
TRANSLATIONAL RESEARCH

Received
2 May 2013

Accepted
4 September 2013

Published
24 September 2013

Correspondence and requests for materials should be addressed to M.O. (otsukamo-tky@umin.ac.jp)

* These authors contributed equally to this work.

Regulation of the expression of the liver cancer susceptibility gene MICA by microRNAs

Takahiro Kishikawa[1]*, Motoyuki Otsuka[1,2]*, Takeshi Yoshikawa[1], Motoko Ohno[1], Akemi Takata[1], Chikako Shibata[1], Yuji Kondo[1], Masao Akanuma[3], Haruhiko Yoshida[1] & Kazuhiko Koike[1]

[1]Department of Gastroenterology, Graduate School of Medicine, The University of Tokyo, Tokyo 113-8655, Japan, [2]Japan Science and Technology Agency, PRESTO, Kawaguchi, Saitama 332-0012, Japan, [3]Division of Gastroenterology, The Institute for Adult Diseases, Asahi Life Foundation, Tokyo 100-0005, Japan.

Hepatocellular carcinoma (HCC) is a threat to public health worldwide. We previously identified the association of a single nucleotide polymorphism (SNP) at the promoter region of the MHC class I polypeptide-related sequence A (MICA) gene with the risk of hepatitis-virus-related HCC. Because this SNP affects MICA expression levels, regulating MICA expression levels may be important in the prevention of HCC. We herein show that the microRNA (miR) 25-93-106b cluster can modulate MICA levels in HCC cells. Overexpression of the miR 25-93-106b cluster significantly suppressed MICA expression. Conversely, silencing of this miR cluster enhanced MICA expression in cells that express substantial amounts of MICA. The changes in MICA expression levels by the miR25-93-106b cluster were biologically significant in an NKG2D-binding assay and an *in vivo* cell-killing model. These data suggest that the modulation of MICA expression levels by miRNAs may be a useful method to regulate HCCs during hepatitis viral infection.

Hepatocellular carcinoma (HCC) is the third most common cause of cancer-related mortality worldwide[1]. Although multiple major risk factors have been identified, such as genetic factors, environmental toxins, alcohol abuse, obesity, and metabolic disorders[2], infection with hepatitis virus B (HBV) or C (HCV) remains the major etiological factor for HCC[1].

Disease progression in HBV-induced or HCV-induced HCC is a multistep phenomenon. The clinical outcomes vary among individuals[1,3,4] because disease progression is influenced by both environmental and genetic risk factors. In terms of genetic susceptibility factors for HCV-induced HCC, we previously identified a single nucleotide polymorphism (SNP) site in the 5′-flanking region of the MICA gene on 6p21.33 (rs2596452) that is strongly associated with progression from chronic hepatitis C to HCC[5]. Individuals with the risk allele A of rs2596452 showed lower serum MICA protein levels[5]. Our subsequent study revealed that the same SNP site was also significantly associated with the risk of HBV-induced HCC[6]. However, interestingly, the risk allele was G in cases of HBV infection, which differed from HCV infection, and the individuals with the risk allele showed increased MICA protein expression levels[6]. Despite the different risk alleles at the same SNP site and inverse association between serum MICA levels and HCC risks in these two etiologies, MICA protein expression levels are significantly associated with susceptibility to HCC in chronic hepatitis viral infection.

MICA is highly expressed on viral-infected and cancer cells and acts as a ligand for NKG2D to activate the antitumor effects of natural killer cells and CD8 T cells[7,8]. This NKG2D-mediated tumor rejection is considered to be effective in the early stages of tumor growth[9–11]. Thus, the expression levels of MICA on the tumor cell surface may determine the antitumor efficacy, and the levels of shedding MICA in serum may act as a decoy of NKG2D to avoid tumor rejection.

Although several stress pathways regulate the transcription of the MICA gene[12,13], cellular microRNAs are suggested to control MICA protein expression via post-transcriptional mechanisms[14,15]. Recently, nucleic-acid-mediated gene therapy has been undergoing clinical trials[16]. Therefore, to target the clinical application of our GWAS results toward prevention of chronic-hepatitis-infection-induced HCC by nucleic-acid-mediated therapy, we determined the regulatory mechanisms of MICA protein expression using miRNA overexpression and miRNA functional silencing.

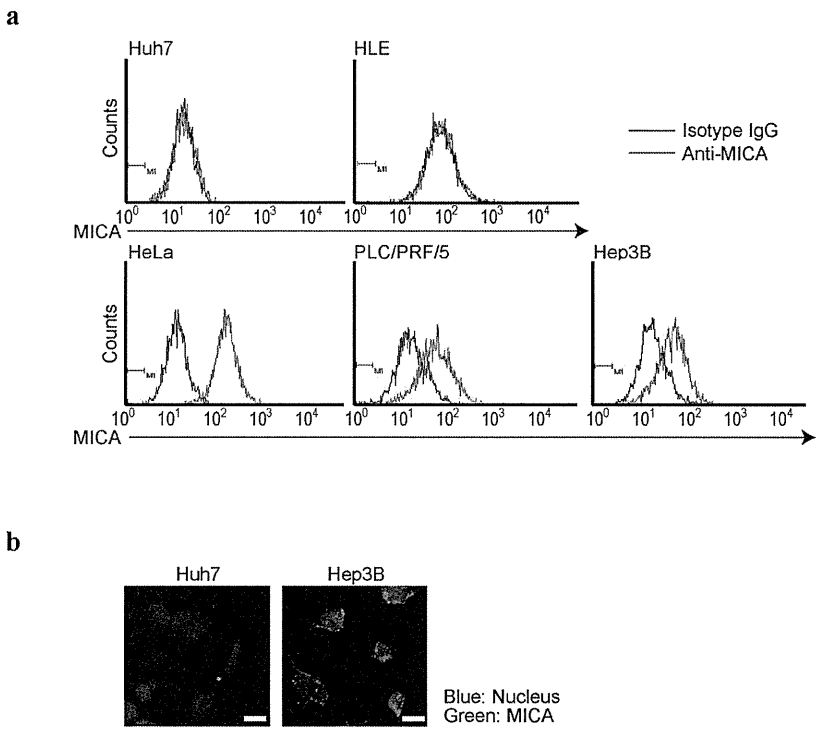

Figure 1 | Expression of MICA protein in HCC cells. (a), Flow cytometry assessment of MICA protein expression in HCC cells (purple lines). Isotype IgG was used for background staining (black lines). HeLa cells were used as the positive control. Representative results from two independent experiments are shown. (b), Immunofluorescence staining for MICA in Huh7 and Hep3B cells. Representative images from two independent experiments are shown. Scale bar, 25 μm.

Results

HCC cell lines differentially express MICA protein. To determine MICA protein levels in HCC cells, four representative HCC cell lines (Huh7, HLE, PLC/PRF/5, and Hep3B cells) underwent flow cytometry to evaluate MICA protein expression because no appropriate antibodies against MICA protein are at present available for western blotting. HeLa cells, which are known to express MICA protein[17], were used as a positive control. Hep3B and PLC/PRF/5 cells expressed substantial MICA protein levels, Huh7 and HLE cells expressed no MICA protein (Figure 1a). This was confirmed by immunocytochemistry using Huh7 and Hep3B cells, which showed staining mainly of cell surfaces (Figure 1b). These results suggest that the MICA protein expression status depends on the cell line examined, even those from the same organ.

The MiR25-93-106b cluster regulates MICA expression. Because upregulation of MICA expression was observed in Dicer-knockdown cells[18], we hypothesized that MICA expression levels may be at least partly regulated by miRNAs. We initially tested miRNAs that might affect MICA expression using reporter constructs into which MICA 3′-untranslated region (3′UTR) sequences were cloned and by transiently overexpressing 76 mature synthetic microRNAs, which were selected on the basis of their hepatic expression level, as in our previous studies[19,20]. Among the microRNAs examined, several may target MICA 3′UTR (Supplementary Figure 1). Among them, we focused on miR93 and miR106b, which were considered to target MICA 3′UTR based partly on the results of our initial miRNA testing described above; in addition, their possible target sequences were identified in the MICA 3′UTR sequences by a computational search using TargetScan 6.0 [21]. Additional reasons that we focused on these two miRNAs were as follows: 1) these miRNAs share the same seed sequences, to which two perfect-match complementary sequences exist in the 3′UTR of MICA (Figure 2a); 2) the target sequences are highly conserved among mammals and are thus likely to be biologically important sites; and 3) these miRNAs are located as a "miR25-93-106b cluster" on human chromosome 7q22.1, and so they may be expressed together under the same transcriptional control. We introduced mutations in the first possible miRNA target sequences of MICA 3′UTR in the reporter constructs (Supplementary Figure 2a); these sequences have a higher likelihood to be target sites, as determined by TargetScan. Co-transfection experiments revealed that reporter activity was suppressed by overexpression of a miR25-93-106b cluster-expressing plasmid (Figure 2b and Supplementary Figure 2b). The overexpression of an unrelated miR (let-7g)-expressing plasmid did not have any significant effects on the reporter activity (Supplementary Figure 2c) and the suppressive effect was lost using constructs with three point mutations in the seed sequences (Figure 2c), suggesting that miR25-93-106b directly targets these sequences and suppresses gene expression.

To confirm these effects, we generated HeLa and Hep3B cell lines that stably expressed the miR25-93-106b-cluster by transducing cells with miR25-93-106b-cluster-expressing lentiviruses (Figure 2d). As expected, the expression of the miR25-93-106b-cluster significantly suppressed MICA protein expression (Figure 2e). However, the expression levels of endogenous miR93 and 106b were not always proportional to the levels of MICA protein expression in the cell lines examined (Supplementary Figure 3). These results suggest that MICA protein expression can be regulated by miR93 and 106b, but that its expression is simultaneously endogenously regulated by other factors (possibly by promoter activities, including epigenetic changes).

Inhibition of miR25-93-106b function increases MICA protein expression. To develop methods of enhancing MICA protein expression levels based on the above results, we examined the

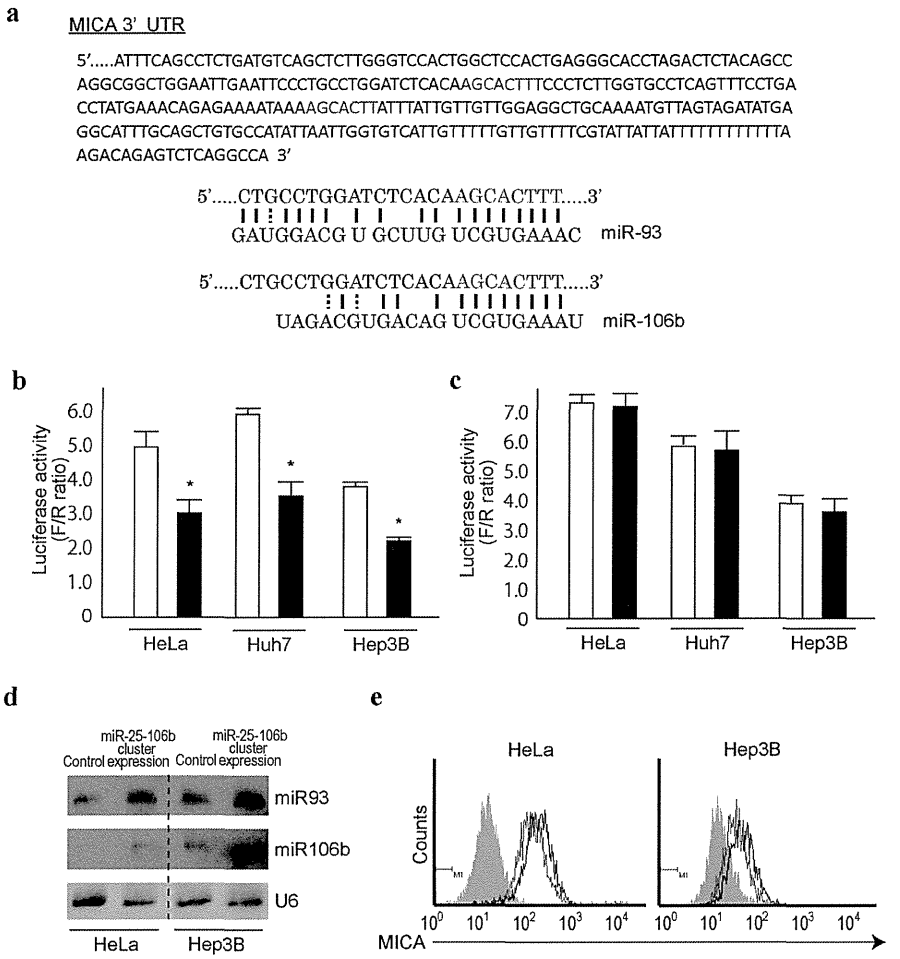

Figure 2 | miR93 and 106b target MICA 3′UTR. (a), Sequences of MICA 3′UTR (upper). Letters in red are the sequences completely matched with the seed regions of miR93 and 106b. The complementarities between the first predicted target in the MICA 3′UTR and miRNA sequences are shown below. (b), (c), Cells were co-transfected with pGL4-TK (renilla luciferase as an internal control), Luc-MICA-3′UTRwt (b) or Luc-MICA-3′UTRmut (c), and either an empty control vector (white bar) or miR25-93-106b-cluster expression plasmid (black bar). Data shows the means ± s.d. of the raw ratios (F/R) obtained by dividing firefly luciferase values with renilla luciferase values of three independent experiments. $*p < 0.05$. (d), miR93 and miR106b expression levels in control and stably miR25-93-106b cluster-expressing cells were determined by northern blotting. U6 levels were used as a loading control. Representative images from two independent experiments are shown. Full-length blot images are available in Supplementary Figure 5. (e), Suppression of MICA expression by overexpression of miRNA93 and 106b. Flow cytometry assessment of MICA protein expression in control (black lines) and stably miR25-93-106b cluster-expressing HeLa and Hep3B cells (red lines). Gray-shaded histograms represent the background staining using isotype IgG. Representative results from two independent experiments are shown.

effects of functional downregulation of miR25-93-106b on MICA expression. We first performed a reporter assay of transient functional silencing of miR25-93-106b using a construct that produces mature anti-sense RNAs designed to silence miR25-93-106b function. As expected, the reporter activities with MICA 3′UTR sequences were enhanced by the functional silencing of miR25-93-106b in HeLa, Hep3B, and Huh7 cells (Figure 3a). However, such effects were not observed using mutant reporter constructs not targeted by those miRNAs (Figure 3b), suggesting that the enhancing effects of the reporter activities were miRNA-dependent.

Next, HeLa, Hep3B, and Huh7 cells were stably transduced with a lentivirus that expresses anti-sense RNAs as described above, and MICA protein expression levels were determined by flow cytometry. Consistent with the reporter assay results, MICA protein expression was increased in HeLa and Hep3B cells by the functional silencing of miR25-93-106b (Figure 3c). However, in Huh7 cells, which express no MICA protein in the normal state, silencing of miR25-93-106b had no effect on MICA protein expression (Figure 3c). These results suggest that MICA protein expression levels can be regulated by modulating miRNA function, albeit only if at least a small quantity of MICA protein is present. In contrast, modulation of miRNA function does not influence MICA protein expression levels when the MICA protein is not expressed, but this could be because there are other forms of regulation at extremely low levels.

MICA protein levels are related to tumor susceptibility to NK cells. To determine the consequences of the modulation of MICA protein expression levels by miRNAs, we first determined the binding ability of NKG2D, a receptor of MICA, using HeLa and Hep3B cells overexpressing the miR25-93-106b cluster or with silencing of miR25-93-106b function. As expected, the levels of NKG2D binding to the cells, theoretically through binding to MICA, were decreased in HeLa and Hep3B cells overexpressing the miR25-93-106b cluster (Figure 4a). On the contrary, the levels of NKG2D binding to the cells were increased in HeLa and Hep3B cells in which miR25-93-106b function had been silenced (Figure 4b).

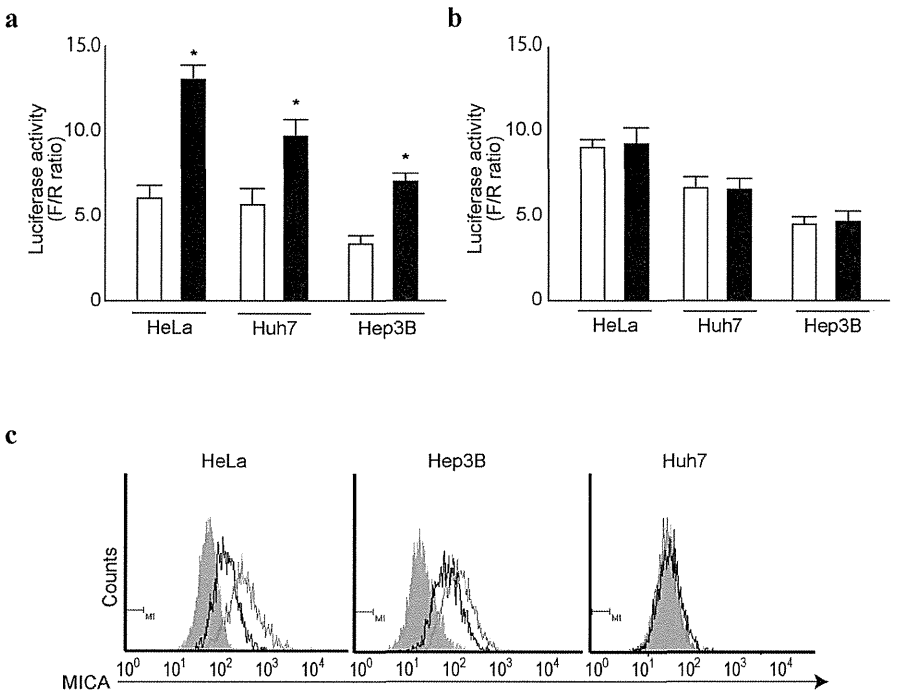

Figure 3 | Silencing of miR25-93-106b cluster enhances MICA expression. (a), (b), Cells were co-transfected with pGL4-TK (internal control), Luc-MICA-3′UTRwt (a) or Luc-MICA-3′UTRmut (b), and either an empty control vector (white bar) or plasmid expressing mature anti-sense sequences of miR25-93-106b cluster (black bar). Data shows the means ± s.d. of the raw ratios (F/R) obtained by dividing firefly luciferase values with renilla luciferase values of three independent experiments. $*p < 0.05$. (c), Enhancement of MICA expression by expression of anti-sense sequences of the miR25-93-106b cluster. Flow cytometry assessment of MICA protein expression in control (black lines) and stably mature anti-sense sequences of miR25-93-106b cluster-expressing cells (green lines). Gray-shaded histograms represent the background staining using isotype IgG. Representative results from three independent experiments are shown.

Next, to determine whether tumor cells with different miRNA-induced MICA protein expression levels exhibited differing susceptibilities to NK-cell-mediated killing *in vivo*, we performed a tumor-clearance assay that measures short-term *in vivo* killing by NK cells[22]. Hep3B control cells, Hep3B cells with miR25-93-106b cluster overexpression, or Hep3B cells with miR25-93-106b and HA-tagged MICA overexpression, labeled with fluorescent DiO, were injected into C57Black6/J mouse tail veins together with an equal number of HeLa cells labeled with Dil (internal reference control). After 5 h, surviving Hep3B and HeLa cells in the lungs were enumerated by flow cytometry. The number of Hep3B cells that had survived divided by the number of HeLa cells that had survived represents the relative killing of Hep3B cells *in vivo*. As shown by the *in vitro* binding assay using NKG2D, the killing rate of Hep3B cells in which miRNA function had been silenced was higher, and that of cells overexpressing miRNAs was lower, than that of control cells. The effects of miRNA overexpression were similar to those obtained in MICA knocked-down Hep3B cells (supplementary Figure 4). Additionally, the lower cell-killing rate in Hep3B cells overexpressing miRNA was antagonized by the co-expression of exogenous MICA protein (Figure 4c), suggesting that the decreased clearance was mediated by reduced MICA expression levels secondary to overexpression of miRNAs. These results suggest that tumor progression and invasion can be regulated by expression or silencing of miRNAs in at least some cells by regulation of MICA expression levels.

Discussion

In this study, we showed that the miR25-93-106b cluster modulates MICA protein expression by HCC cells. Because our previous GWAS analyses identified that MICA is the critical gene determining HCC susceptibility in patients with chronic hepatitis infection[5,6], the herein-described methods of modulating MICA expression may be useful for developing novel methods of prevention and therapeutics against HCCs.

MICA is a membrane protein that acts as a ligand for NKG2D to activate innate anti-tumor effects through natural killer and $CD8^+$ cells[7]. Our previous GWAS study showed that a risk allele at the SNP in the MICA promoter region was significantly associated with the susceptibility of HCV-induced HCC as well as with lower serum MICA levels. Although polymorphisms at the same SNP site were also associated with HBV-induced HCC, the risk allele determining the susceptibility of HCC was somehow different from that in HCV-induced HCC. While the reason why different MICA gene variations act as risk alleles at the same SNP site between HBV- and HCV-induced HCC has not been elucidated, it is assumed that changes in the membrane-bound MICA and soluble MICA levels due to differences in post-translational processing according to virus type may affect the risk allele results. In any case, because the importance of the regulation of MICA expression levels to prevent development of HCC due to chronic hepatitis viral infection cannot be denied, the regulation of MICA levels by microRNAs as shown here may be useful for the development of preventive methods of preventing HCC development during chronic hepatitis infection.

While several cellular signaling pathways lead to upregulation of MICA[12,13], we used microRNAs to regulate the expression levels of MICA in this study. As shown by the results of our GWAS analyses, which found that the polymorphisms in the promoter region of MICA are associated with changes in the sMICA levels[5,6], promoter activities of the MICA gene also have significant effects on MICA expression levels[23]. Our results showed that miR93 and 106b expression levels were not always correlated with those of MICA in HCC cell lines, suggesting that the regulation of MICA expression is not solely

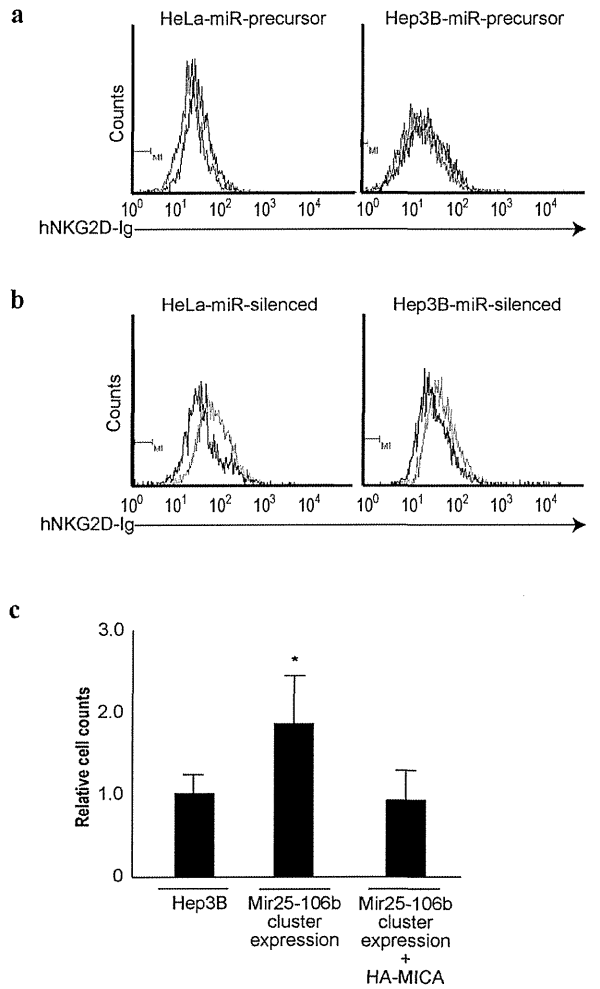

Figure 4 | NKG2D binding levels change in proportion to MICA expression levels. (a), (b), Flow cytometry of human IgG-fused NKG2D binding to the control (black lines), miR25-93-106b cluster-expressing cells (red lines) (a), and mature anti-sense sequences of miR25-93-106b cluster-expressing cells (green lines) (b). Representative results from three independent experiments are shown. (c), *In vivo* killing of DiO-labeled Hep3B and Dil-labeled HeLa cells (internal control cells) injected together into the tail veins of six mice in each group. Fluorescence intensities were quantified by flow cytometry as the ratio of Hep3B to HeLa cells in the lungs. The data from control Hep3B cells were set as 1.0. Data represent the means ± s.d. of three independent experiments. $*p < 0.05$.

dependent on miRNAs. In addition, in cells with no endogenous MICA expression, such as Huh7 cells, modulation of microRNA expression had no effect on the regulation of MICA expression. This suggests that at least low-level endogenous expression, which may be determined by promoter activities, are needed for regulation by miRNA. Therefore, changes in promoter activities and epigenetic changes in the MICA gene should also be determined. This will facilitate application of the regulatory function of miRNAs reported here.

One class of antisense oligonucleotides, namely locked nucleic acids, can be used to sequester microRNAs in the liver of various animals, including humans[16,24,25]. A clinical trial targeting miR-122 with the anti-miR-122 oligonucleotides miravirsen, the first miRNA-targeted drug, is underway for the treatment of HCV infection[16]. Thus, nucleic-acid-mediated gene therapy is becoming a realistic option. Modulation of MICA expression levels by such nucleic-acid-mediated therapy based on the results presented herein may also be a promising option for prevention and/or therapy of HCC.

In summary, we have shown that the miR25-93-106b cluster can be used to modulate MICA expression levels in HCC cells. Based on our GWAS results and associated studies, regulation of MICA protein expression levels is crucial to prevent the development of HCC during chronic hepatitis viral infection. It is important to identify the other factors that regulate MICA transcriptional activities as well as the post-translational processes and their association with susceptibility to HCCs. That said, miRNA regulation of MICA expression as shown here may facilitate regulation of the host innate immune system in an HCC-suppressive manner during chronic hepatitis viral infection.

Methods

Cell culture. The human HCC cell lines Huh7, HLE, PLC/PRF/5, and Hep3B were obtained from the Japanese Collection of Research Bioresources (JCRB, Osaka, Japan). The human cervical cancer cell line HeLa was obtained from the American Type Culture Collection (ATCC, Rockville, MD). All cells were maintained in Dulbecco's modified Eagle's medium supplemented with 10% fetal bovine serum.

Mouse. Experimental protocols were approved by the Ethics Committee for Animal Experimentation at the Graduate School of Medicine, the University of Tokyo and the Institute for Adult Disease, Asahi Life Foundation, Japan and conducted in accordance with the Guidelines for the Care and Use of Laboratory Animals of the Department of Medicine, the University of Tokyo, and the Institute for Adult Disease, Asahi Life Foundation.

Flow cytometry. Cells were hybridized with anti-MICA (1 : 500; R&D Systems, Minneapolis, MN) and isotype control IgG (1 : 500; R&D Systems) in 5% BSA/1% sodium azide/PBS for 1 h at 4°C. After washing, cells were incubated with goat anti-mouse Alexa 488 (1 : 1000; Molecular Probes, Eugene, OR) for 30 min. Flow cytometry was performed and data analyzed using Guava Easy Cyte Plus (GE Healthcare, Little Chalfont, UK).

Reporter plasmid construction, transient transfections, and luciferase assays. The reporter plasmid for the analysis of the effects of miRNAs on MICA 3′UTR were constructed by subcloning the MICA 3′UTR sequences from pLightSwitch-MICA 3UTR (SwitchGear Genomics, Menlo Park, CA) into the pGL4.50 vector (Promega, Madison, WI) at the *FseI* site by the In-Fusion method (Clontech, Mountain View, CA) to insert the MICA 3′UTR sequences into the 3′-UTR of the firefly luciferase gene, which was under the control of the CMV promoter. The sequences of the primers were 5′-CTA GAG TCG GGG CGG CG GCC ATT TCA GCC TCT GAT GTC AGC-3′ and 5′-GTC TGC TCG AAG CGG CCG GCC TGG CCT GAG ACT CTG TCT TAA-3′. The resultant plasmid (Luc-MICA 3′UTRwt) was used as a template for the construction of mutant reporter plasmid (Luc-MICA 3′UTRmut), which carries three point mutations in the seed sequences of miR93 and 106b in the MICA 3′UTR, itself generated by a Quik Change II XL Site-directed Mutagenesis Kit (Stratagene, Heidelberg, Germany) according to the manufacturer's instructions. Transient transfection and reporter assays were performed as described previously[26].

Lentiviral constructs, viral production, and transduction. To generate a neomycin-resistant miR25-93-106b cluster-expressing lentiviral construct, copGFP in the pmiRNA25-93-106b cluster-expressing plasmid (System Biosciences, Mountain View, CA) was replaced with a neomycin resistant gene, which was subcloned from the pCDH-Neo vector (System Biosciences), at the *FseI* site. The primers used were 5′-GCT ACC GCT ACG AGG CCG GCC CAT GAT TGA ACA AGA TGG ATT GCA-3′ and 5′-TCG CCG ATC ACG CGG CCG GCC TCA GAA GAA CTC GTC AAG AAG GC-3′. To remove the copGFP region from pmiRZIP25-93-106b (System Biosciences), a construct expressing mature anti-sense sequences of the miR25-93-106b cluster, sequences coding the GFP gene were removed by excision with *Xba*I and *Pst*I sites followed by connecting the cut ends with annealed oligonucleotides (5′-CTA GAC GCC ACC ATG CTG CA-3′ and 5′-GCA TGG TGG CGT-3′) to maintain the coding frame and the expression of the downstream puromycin-resistance gene. To generate HA-tagged MICA protein overexpressing the lentiviral construct, MICA cDNA was amplified by PCR using a Halo-tag-MICA–expressing plasmid (Promega, Madison, WI) as a template and cloned into a pCDH-puro vector (System Biosciences) at the *Not*I site. The primer sequences used were 5′-ATC GGA TCC GCG GCC GCA CCA TGT ACC CAT ACG ATG TTC CAG ATT ACG CTA TGG GGC TGG GCC CGG TC-3′ and 5′-AGA TCC TTC GCG GCC GCT TAG GCG CCC TCA GTG GAG C-3′. Let-7g precursor expressing plasmid was generated by inserting about 1,000 bp long PCR product around the let-7g genomic region into pCDH-puro vector using *Xba*1 and *Not*1 sites. The production and concentration of lentiviral particles were described previously[27]. shRNA against MICA-producing lentiviral particles with puromycin resistant gene were purchased from SantaCruz Biotechnology (sc-4924-V, Dallas, TX). Cells were transduced with lentiviruses using

polybrene (EMD Millipore, Billerica, MA). The selections were performed with 400 μg/mL G418 and 2 μg/mL (HeLa) or 6 μg/mL (Hep3B) puromycin.

Immunocytochemistry. Cells on two-well chamber slides were fixed with 4% paraformaldehyde. Fixed cells were probed with the primary MICA antibody (R&D Systems) for 1 h after blocking with 5% normal goat serum for 30 min. Cells probed with the MICA antibody were incubated with the secondary Alexa Fluor 488 goat anti-mouse antibody (Molecular Probes) for 30 min. Slides were mounted using VectaShield with DAPI (Vector Labs, Burlingame, CA).

Northern blotting of miRNAs. Northern blotting of miRNAs was performed as described previously[27]. Briefly, total RNA was extracted using TRIzol Reagent (Invitrogen, Carlsbad, CA) according to the manufacturer's instructions. Ten micrograms of RNA were resolved in denaturing 15% polyacrylamide gels containing 7 M urea in 1 × TBE and then transferred to a Hybond N+ membrane (GE Healthcare) in 0.25 × TBE. Membranes were UV-crosslinked and prehybridized in hybridization buffer. Hybridization was performed overnight at 42°C in ULTRAhyb-Oligo Buffer (Ambion) containing a biotinylated probe specific for miR93 (cta cct gca cga aca gca ctt tg) and 106b (atc tgc act gtc agc act tta), which had previously been heated to 95°C for 2 min. Membranes were washed at 42°C in 2 × SSC containing 0.1% SDS, and the bound probe was visualized using a BrightStar BioDetect Kit (Ambion). Blots were stripped by boiling in a solution containing 0.1% SDS and 5 mM EDTA for 10 min prior to rehybridization with a U6 probe (cac gaa ttt gcg tgt cat cct t).

miRNA library screening. To screen for miRNAs that target MICA 3′-UTR, synthetic miRNA mimics and reporter constructs were used as described previously[19,20]. Seventy-six types of synthetic mature miRNAs that are highly expressed in the liver[28] were custom-made (B-Bridge, Tokyo, Japan) and transfected by RNAi Max (Life Technologies, Carlsbad, CA) into Huh7 cells in 96-well plates that had been transfected 24 h before with Luc-MICA 3′UTRwt. The cells were then incubated for another 24 h. As negative controls, oligonucleotides of artificial sequences were applied[19]. The luciferase activities were measured using a GloMax 96 Microplate Luminometer (Promega). The experiments were performed in duplicate.

NKG2D binding assay. Cells were incubated with 4 μg of recombinant human NKG2D fused to human IgG1 Fc chimera protein. After washing, cells were incubated with an Alexa488-conjugated affinity purified F(ab')2 fragment of goat anti-human IgG (Jackson ImmunoResearch Laboratories, West Grove, PA). As a negative control, cells were incubated with only Alexa488 anti-human IgG. The intensity of the fluorescence was determined by flow cytometry.

***In vivo* cell-killing assay.** Hep3B cells and HeLa cells were labeled with the fluorescent dye VybrantDiO and DiI (Molecular Probes), respectively. Cells were mixed at a density of 2×10^7 in 1-ml PBS, and 200 μl was injected into the tail vein. Five hours later, lungs were collected, and single-cell suspensions were collected using a cell strainer. Fluorescence was assayed by flow cytometry, and the ratio of the experimental Hep3B cells to HeLa cells (internal control) was calculated.

Statistical analysis. Statistically significant differences between groups were determined using Student's *t*-test when variances were equal. When variances were unequal, Welch's *t*-test was used instead. *P*-values of < 0.05 were considered to indicate statistical significance.

1. El-Serag, H. B. Epidemiology of viral hepatitis and hepatocellular carcinoma. *Gastroenterology* **142**, 1264–1273 (2012).
2. Sherman, M. Hepatocellular carcinoma: New and emerging risks. *Dig Liver Dis* **42**, S215–222 (2010).
3. Arzumanyan, A., Reis, H. M. & Feitelson, M. A. Pathogenic mechanisms in HBV- and HCV-associated hepatocellular carcinoma. *Nat Rev Cancer* **13**, 123–135 (2013).
4. Urabe, Y. *et al.* A genome-wide association study of HCV-induced liver cirrhosis in the Japanese population identifies novel susceptibility loci at the MHC region. *J Hepatol* (2013).
5. Kumar, V. *et al.* Genome-wide association study identifies a susceptibility locus for HCV-induced hepatocellular carcinoma. *Nat Genet* **43**, 455–458 (2011).
6. Kumar, V. *et al.* Soluble MICA and a MICA variation as possible prognostic biomarkers for HBV-induced hepatocellular carcinoma. *PLoS One* **7**, e44743 (2012).
7. Maccalli, C., Scaramuzza, S. & Parmiani, G. TNK cells (NKG2D+ CD8+ or CD4+ T lymphocytes) in the control of human tumors. *Cancer Immunol Immunother* **58**, 801–808 (2009).
8. Jinushi, M. *et al.* Impairment of natural killer cell and dendritic cell functions by the soluble form of MHC class I-related chain A in advanced human hepatocellular carcinomas. *J Hepatol* **43**, 1013–1020 (2005).
9. Diefenbach, A., Jensen, E. R., Jamieson, A. M. & Raulet, D. H. Rae1 and H60 ligands of the NKG2D receptor stimulate tumour immunity. *Nature* **413**, 165–171 (2001).
10. Hayakawa, Y. Targeting NKG2D in tumor surveillance. *Expert Opin Ther Targets* **16**, 587–599 (2012).
11. Guerra, N. *et al.* NKG2D-deficient mice are defective in tumor surveillance in models of spontaneous malignancy. *Immunity* **28**, 571–580 (2008).
12. Bauer, S. *et al.* Activation of NK cells and T cells by NKG2D, a receptor for stress-inducible MICA. *Science* **285**, 727–729 (1999).
13. Eleme, K. *et al.* Cell surface organization of stress-inducible proteins ULBP and MICA that stimulate human NK cells and T cells via NKG2D. *J Exp Med* **199**, 1005–1010 (2004).
14. Yadav, D., Ngolab, J., Lim, R. S., Krishnamurthy, S. & Bui, J. D. Cutting edge: down-regulation of MHC class I-related chain A on tumor cells by IFN-gamma-induced microRNA. *J Immunol* **182**, 39–43 (2009).
15. Stern-Ginossar, N. & Mandelboim, O. An integrated view of the regulation of NKG2D ligands. *Immunology* **128**, 1–6 (2009).
16. Janssen, H. L. *et al.* Treatment of HCV Infection by Targeting MicroRNA. *N Engl J Med* **368**, 1685–94 (2013).
17. Salih, H. R., Rammensee, H. G. & Steinle, A. Cutting edge: down-regulation of MICA on human tumors by proteolytic shedding. *J Immunol* **169**, 4098–4102 (2002).
18. Tang, K. F. *et al.* Decreased Dicer expression elicits DNA damage and up-regulation of MICA and MICB. *J Cell Biol* **182**, 233–239 (2008).
19. Takata, A. *et al.* MicroRNA-22 and microRNA-140 suppress NF-κB activity by regulating the expression of NF-κB coactivators. *Biochem Biophys Res Commun* **411**, 826–831 (2011).
20. Yoshikawa, T. *et al.* Silencing of microRNA-122 enhances interferon-a signaling in the liver through regulating SOCS3 promoter methylation. *Sci. Rep.* **2**, 637 (2012).
21. Lewis, B. P., Burge, C. B. & Bartel, D. P. Conserved seed pairing, often flanked by adenosines, indicates that thousands of human genes are microRNA targets. *Cell* **120**, 15–20 (2005).
22. Gazit, R. *et al.* Lethal influenza infection in the absence of the natural killer cell receptor gene Ncr1. *Nat Immunol* **7**, 517–523 (2006).
23. Lo, P. H. *et al.* Identification of a Functional Variant in the MICA Promoter Which Regulates MICA Expression and Increases HCV-Related Hepatocellular Carcinoma Risk. *PLoS One* **8**, e61279 (2013).
24. Lanford, R. E. *et al.* Therapeutic silencing of microRNA-122 in primates with chronic hepatitis C virus infection. *Science* **327**, 198–201 (2010).
25. Elmén, J. *et al.* LNA-mediated microRNA silencing in non-human primates. *Nature* **452**, 896–899 (2008).
26. Kojima, K. *et al.* MicroRNA122 is a key regulator of α-fetoprotein expression and influences the aggressiveness of hepatocellular carcinoma. *Nat Commun* **2**, 338 (2011).
27. Takata, A. *et al.* MicroRNA-140 acts as a liver tumor suppressor by controlling NF-κB activity by directly targeting DNA methyltransferase 1 (Dnmt1) expression. *Hepatology* **57**, 162–170 (2013).
28. Krützfeldt, J. *et al.* Silencing of microRNAs in vivo with 'antagomirs'. *Nature* **438**, 685–689 (2005).

Acknowledgments

This work was supported by Grants-in-Aid from the Ministry of Education, Culture, Sports, Science and Technology, Japan (#25293076, #25460979, and #24390183) (to M.Otsuka, Y.K. and K.K.), by Health Sciences Research Grants of The Ministry of Health, Labour and Welfare of Japan (to K.K.), and by grants from the Okinaka Memorial Institute for Medical Research, the Liver Forum in Kyoto, and the Princess Takamatsu Cancer Research Fund (to M.Otsuka).

Author contributions

T.K., M. Otsuka and K.K. planned the research and wrote the paper. T.K., M. Otsuka, T.Y., M. Ohno, A.T., C.S. and Y.K. performed the majority of the experiments. M.A. and H.Y. supported several experiments and analyzed the data. K.K. supervised the entire project.

Additional information

Supplementary information accompanies this paper at http://www.nature.com/scientificreports

Competing financial interests: The authors declare no competing financial interests.

How to cite this article: Kishikawa, T. *et al.* Regulation of the expression of the liver cancer susceptibility gene MICA by microRNAs. *Sci. Rep.* **3**, 2739; DOI:10.1038/srep02739 (2013).

Hepatology Research

Hepatology Research 2013; 43: 596–604 doi: 10.1111/j.1872-034X.2012.01115.x

Original Article

Fibrosis score consisting of four serum markers successfully predicts pathological fibrotic stages of chronic hepatitis B

Kenji Ikeda,[1,2] Namiki Izumi,[3] Eiji Tanaka,[7] Hiroshi Yotsuyanagi,[4] Yoshihisa Takahashi,[5] Junichi Fukushima,[6] Fukuo Kondo,[5] Toshio Fukusato,[5] Kazuhiko Koike,[4] Norio Hayashi[8] and Hiromitsu Kumada[1,2]

[1]*Department of Hepatology, Toranomon Hospital,* [2]*Okinaka Memorial Institute for Medical Research,* [3]*Department of Gastroenterology, Musashino Red Cross Hospital,* [4]*Department of Gastroenterology, Tokyo University of Medicine,*[5]*Department of Pathology, Teikyo University School of Medicine,* [6]*Department of Pathology, NTT Medical Center Tokyo, Tokyo,* [7]*Department of Gastroenterology, Shinshu University of Medicine, Matsumoto, and* [8]*Department of Gastroenterology, Kansai-Rosai Hospital, Hyogo, Japan*

Aim: In order to evaluate and judge a fibrotic stage of patients with chronic hepatitis B, multivariate regression analysis was performed using multiple fibrosis markers.

Method: A total of 227 patients from seven hepatology units and institutes were diagnosed by needle biopsy as having chronic liver disease caused by hepatitis B virus. Twenty-three variables and their natural logarithmic transformation were employed in the multivariate analysis. Multiple regression function was generated from data of 158 patients in one hospital, and validation was performed using the other data of 69 patients from six other hospitals.

Results: After stepwise variable selection, multivariate regression analysis finally obtained the following function: $z = 1.40 \times ln$ (type IV collagen 7S) (ng/mL) $- 0.017 \times$ (platelet count) ($\times 1000^3/mm^3$) $+ 1.24 \times ln$ (tissue inhibitor of matrix metalloproteinase-2) (ng/mL) $+ 1.19 \times ln$ (α-2-macroglobulin) (mg/dL) $- 9.15$. Median values of fibrosis scores of F1 ($n = 73$), F2 ($n = 42$), F3 ($n = 31$) and F4 stages ($n = 12$) were calculated as 0.95, 2.07, 2.98 and 3.63, respectively. Multiple regression coefficient and coefficient of determination were 0.646 and 0.418, respectively. Validation with patient data from other institutions demonstrated good reproducibility of fibrosis score for hepatitis B (FSB), showing 1.33 in F1 ($n = 27$), 2.20 in F2 ($n = 20$), 3.11 in F3 ($n = 20$) and 5.30 in F4 ($n = 2$), respectively.

Conclusion: A concise multiple regression function using four laboratory parameters successfully predicted pathological fibrosis stage of patients with hepatitis B virus infection.

Key words: chronic hepatitis, hepatitis B virus, liver cirrhosis, liver fibrosis, multiple regression analysis, stage

INTRODUCTION

WHEN HEPATITIS B virus (HBV)-related chronic liver disease is found by biochemical and virological examination, liver biopsy can establish the definitive diagnosis of chronic hepatitis and its fibrotic staging. Although these pathological procedures are reliable and informative both in diagnosis and treatment, they sometimes require medical invasion and financial costs, including the risk of bleeding from needle puncture, some pain experienced during the procedure and hospital stays of a few days. The pathological examination is, therefore, rarely performed repeatedly in a short period of time, unless disease activity is severe or progression of liver disease is highly suspected. Recently, many authors described the usefulness of ultrasonographic elastography and multiple resonance imaging technology in the estimation of staging of chronic hepatitis and cirrhosis.[1–5] These ways of estimation using the imaging apparatuses seem truly useful for current patients, but they cannot evaluate and compare with past fibrotic states of patients retrospectively. Moreover,

Correspondence: Dr Kenji Ikeda, Department of Hepatology, Toranomon Hospital, 2-2-2 Toranomon, Minato-ku, Tokyo, 105-8470, Japan. Email: ikedakenji@tora.email.ne.jp
Received 6 May 2012; revision 17 September 2012; accepted 4 October 2012.

the same apparatus for elastometry will not be available for repeated measurement for a follow-up examination, for example, several years later.

In spite of the accuracy of biopsy and convenience of elastography in chronic liver disease, clinical diagnosis based on biochemistry and hematology is still indispensable for the daily practice of many patients with HBV-related liver disease. Recently, several studies were published about estimation of hepatitis stages, using one or more serum biomarkers. Discriminant functions or multivariate analyses demonstrated that approximately 60–90% of patients with chronic hepatitis B were correctly classified as having mild hepatitis and severe hepatitis with advanced fibrosis.[2,6–13] Up to the present time, however, the usefulness of the discriminant functions are less valuable for a few reasons. First, these functions were made for the purpose of discrimination of severe hepatic fibrosis from mild fibrosis, and four histological classifications (F1–F4) were neglected in almost of the studies. Second, some studies analyzed both hepatitis B and hepatitis C virus infection, although the significance and actual values of each liver function test in the evaluation of the severity of liver disease were not similar among each viral hepatitis and alcoholic liver disease. Third, biochemical markers for liver fibrosis (e.g. hyaluronic acid, type IV collagen, procollagen III peptide)[14–16] were not always included in those previous studies.

We tried to generate a function estimating fibrotic stages of HBV-related chronic hepatitis, which were objectively diagnosed by liver biopsy. The purpose of this study is, therefore, to make a reliable multiple regression function and to obtain practical coefficients for significant variables also using fibrosis markers.

METHODS

Patients

A TOTAL OF 273 Japanese patients with chronic hepatitis B were recruited for the study from seven hospitals in Japan: Toranomon Hospital, Hiroshima University Hospital (K. Chayama, M.D.), Ehime University Hospital (M. Onji, M.D.), Musashino Red Cross Hospital (N. Izumi, MD), Shishu University Hospital (E. Tanaka, M.D.), Showa University Hospital (M. Imawari, M.D.) and Osaka University Hospital (T. Takehara, M.D.). Inclusion criteria for this study were: (i) positive hepatitis B surface antigen for more than 6 months; (ii) persistent or intermittent elevation in aspartate aminotransferase (AST)/alanine aminotransferase (ALT) levels; and (iii) liver biopsy showing chronic hepatitis (F1–F4). We excluded those patients with overt alcoholic liver disease or fatty liver, association of other types of liver disease (e.g. hepatitis C, primary biliary cirrhosis, autoimmune hepatitis), or those associated with hepatocellular carcinoma or other malignancy. Among the patients, 244 patients fulfilled the conditions for the study: complete demographic data, basic laboratory data of hematology and biochemistry, required liver biopsy specimens, and sufficient amount of frozen sera. Also, we excluded additional 17 patients with eventual histological diagnosis as F0 stage.

Finally, a total of 227 patients who were diagnosed as having chronic hepatitis or cirrhosis (F1–F4) were analyzed for the following hematological, biochemical and histopathological examination. There were 172 males and 55 females aged 16–70 years (median, 39 years).

All the patients presented written informed consent in individual hospitals and medical centers, and the study was approved in each ethical committee.

Hematological and biochemical examination

Hematological and standard biochemical evaluation had been performed in each medical institution: white blood cells, red blood cells, hemoglobin, platelets, total bilirubin, AST, ALT, AST/ALT ratio (AAR), γ-glutamyl transpeptidase (γ-GTP), total protein, albumin and γ-globulin.

Special biochemical examinations including "fibrosis markers" were carried out using stored frozen sera at −20°C or lower: α-2-macroglobulin, haptoglobin concentration, haptoglobin typing, apolipoprotein A1, hyaluronic acid, tissue inhibitor of matrix metalloproteinase (TIMP)-1, TIMP-2, procollagen III peptide and type IV collagen 7S.

Histological diagnosis of chronic hepatitis and cirrhosis

All the 227 cases fulfilled required standards of histological evaluation: sufficient length of specimen, hematoxylin–eosin staining, and at least one specimen with fiber staining. Four independent pathologists (Y. T., J. F., F. K. and T. F.), who were not informed of patients' background and laboratory features except for age and sex, evaluated the 227 specimens regarding the stages of fibrosis and activity. Pathological classification of chronic hepatitis staging was based on Desmet *et al.*[17]

Before judgment of histological staging of individual specimens, the pathologists discussed the objective and reproducible judgment of pathological diagnosis of

hepatitis. They made a panel about obvious criteria using typical microscopic pictures for each stage, and it was always referred to during the procedure of pathological judgment. When inconsistent results were found in the diagnosis of hepatitis stage among the pathologists, the final judgment accepted majority rule among them.

Statistical analysis

Non-parametric procedures were employed for the analysis of background characteristics and laboratory data among patients in each stage, including Mann–Whitney *U*-test, Kruskal–Wallis test and χ^2-test.

The normality of the distribution of the data was evaluated by a Kolmogorov–Smirnov one-sample test. Because certain variables partly did not conform to a normal distribution, natural logarithmic transformation of bilirubin, AST, ALT, γ-GTP, α-2-macroglobulin, hyaluronic acid, type IV collagen 7S and TIMP-2 were also analyzed in the following calculation. The natural logarithmic transformation of the results yielded a normal distribution or symmetrical distribution for all the analyzed factors. After the procedures, the following multiple regression analysis became rationally robust against deviations from normal distribution. In order to avoid introducing into the model any variables that were mutually correlated, we checked the interaction between all pairs of the variables by calculating variance inflation factors. Of the highly correlated variables, less significant factors were removed from the viewpoint of multicollinearity.

Multivariate regression analysis was performed using 158 patient data from Toranomon Hospital (training dataset) to generate a training data of predicting function. We used a stepwise method for selection of informative subsets of explanatory variables in the model. Multiple regression coefficient and coefficient of determination were also taken into account in the selection of variables. Next, we validated the obtained predictive function using the remaining 69 patient data from the other six liver institutions (validation dataset).

A *P*-value of less than 0.05 with two-tailed test was considered to be significant. Data analysis was performed using the computer program SPSS ver. 19.[18]

For evaluation of the efficiency and usefulness of obtained function for fibrosis estimation, we compared various fibrosis scores for hepatitis B and C, including AAR,[19] AST-to-platelet ratio index (APRI),[20] FIB-4,[21] FibroTest[22] and discrimination function of cirrhosis from hepatitis in Japanese patients.[23]

RESULTS

Pathological diagnosis

FOUR PATHOLOGISTS INDEPENDENTLY judged the fibrotic stages and inflammatory activity for 227 specimens of chronic hepatitis/cirrhosis caused by HBV. One hundred patients (44.1%) had a fibrosis stage of F1, 62 (27.3%) F2, 51 (22.5%) F3 and 14 (6.2%) F4. In the subgroup of the 158 patients in the training group, judgment as F1 was made in 73 cases, F2 in 42, F3 in 31 and F4 in 12. Of the 69 patients in the validation group, judgment as F1 was made in 27, F2 in 20, F3 in 20 and F4 in two.

According to hepatitis activity classification, A0 was found in five (2.2%), A1 in 100 (44.1%), A2 in 107 (47.1%) and A3 in 15 (6.6%).

Laboratory data of each hepatitis stage in the training group

There were 124 men and 34 women with a median age of 39 years ranged 16–70 years. Laboratory data of 158 patients in the training group are shown in Table 1. Although several individual items were well correlated with the severity of hepatic fibrosis, significant overlap values were noted among F1–F4 stages: platelet count, γ-globulin, α-2-macroglobulin, haptoglobin, hyaluronic acid, TIMP-2 and type IV collagen 7S.

Significant variables serving staging of hepatitis

Univariate analyses using trend analysis with the Cochran–Armitage method showed that the fibrotic stage of chronic hepatitis B (FSB) was significantly correlated with platelet count (Spearman: $r = -0.45$, $P < 0.001$), γ-GTP ($r = 0.19$, $P = 0.017$), γ-globulin ($r = 0.29$, $P < 0.001$), α-2-macroglobulin ($r = 0.32$, $P < 0.001$), hyaluronic acid ($r = 0.36$, $P < 0.001$), TIMP-2 ($r = 0.16$, $P = 0.043$), procollagen III peptide ($r = 0.30$, $P < 0.001$) and type IV collagen 7S ($r = 0.55$, $P < 0.001$).

Regression function generated from training patient group

After stepwise variable selection, multivariate regression analysis finally obtained the following function: $z = 1.40 \times ln$ (type IV collagen 7S) (ng/mL) $- 0.017 \times$ (platelet count) ($\times 1000^3/mm^3$) $+ 1.24 \times ln$ (TIMP-2) (ng/mL) $+ 1.19 \times ln$ (α-2-macroglobulin) (mg/dL) $-$ 9.15. Median values of the fibrosis score of F1 ($n = 73$), F2 ($n = 42$), F3 ($n = 31$) and F4 stages ($n = 12$) were calculated as 0.95, 2.07, 2.98 and 3.63, respectively

Table 1 Demography and laboratory data of 158 patients in training group

	F1 ($n = 73$)	F2 ($n = 42$)	F3 ($n = 31$)	F4 ($n = 12$)
Demographics				
Men : women	58:15	33:9	23:8	10:2
Age (median, range)	36 (16–70)	39.5 (18–66)	39 (25–64)	43 (32–59)
Laboratory data (median, range)				
WBC (×1000/mm^3)	5.4 (2.5–10.6)	5.1 (2.4–8.7)	4.9 (3.0–8.7)	4.1 (3.7–6.6)
Hemoglobin (g/dL)	15.3 (10.3–18.8)	15.4 (12.5–17.9)	15.2 (11.5–17.2)	14.45 (12.1–18.2)
Platelet (×1000/mm^3)	204 (124–341)	173 (82–308)	155 (96–220)	130 (86–230)
Albumin (g/dL)	4.1 (3.2–4.9)	4.0 (3.2–5.1)	4.0 (3.3–4.9)	3.95 (3.4–4.6)
Bilirubin (mg/dL)	0.8 (0.2–1.7)	0.8 (0.3–2.3)	0.9 (0.4–5.4)	0.85 (0.6–2.3)
AST (IU/L)	48 (16–450)	55 (17–588)	54 (17–1446)	76.5 (27–396)
ALT (IU/L)	102 (10–839)	90 (12–886)	85 (19–2148)	89 (18–809)
γ-GTP (IU/L)	37 (7–247)	55 (8–687)	44 (14–564)	69 (33–262)
γ-Globulin (g/dL)	1.29 (0.78–2.11)	1.495 (0.62–3.20)	1.43 (0.90–2.30)	1.735 (0.92–2.47)
γ-Globulin (%)	17.3 (10.8–26.1)	19.3 (8.5–35.6)	19.9 (12.9–28.6)	22.55 (13.9–30.2)
α-2-Macroglobulin (mg/dL)	226 (116–446)	276 (148–495)	261 (202–565)	286.5 (166–425)
Haptoglobin (mg/dL)	77 (<5–318)	59 (<5–238)	61 (<5–151)	48.5 (<5–145)
Apolipoprotein A-I (mg/dL)	134 (89–212)	143 (78–250)	133 (87–189)	125 (73–169)
Hyaluronic acid (μg/L)	16 (<5–130)	32.5 (<5–204)	38 (<5–418)	49 (24–335)
TIMP-1 (ng/mL)	168 (93–271)	172 (116–314)	157 (119–365)	192 (145–365)
TIMP-2 (ng/mL)	80 (41–135)	80.5 (35–121)	92 (38–251)	85.5 (70–123)
Procollagen III peptide (U/mL)	0.75 (0.53–1.90)	0.835 (0.45–1.20)	0.89 (0.58–2.50)	1.05 (0.71–2.20)
Type IV collagen 7S (ng/ml)	4.0 (2.7–7.7)	4.6 (2.6–9.6)	5.6 (2.3–15.0)	7.2 (4.2–14.0)

ALT, alanine aminotransferase; AST, aspartate aminotransferase; γ-GTP, γ-glutamyl transpeptidase; TIMP, tissue inhibitor of matrix metalloproteinase; WBC, white blood cells.

(Fig. 1). The multiple regression coefficient and coefficient of determination were 0.646 ($P < 0.001$) and 0.418 ($P < 0.001$), respectively.

Because the generated regression function was obtained by multivariate analysis with stepwise variable selection, several variables were removed from the function due to multicollinearity among them. Mutual correlation among the fibrosis predictors are shown in Table 2.

A 28-year-old man of F1 fibrotic stage (Fig. 2a) had a serum type IV collagen concentration of 4.4 ng/mL, platelet 221×10^3 count/mm^3, TIMP-2 75 ng/mL and α-2-macroglobulin 226 mg/dL. The regression function provided a fibrosis score of 0.99. Another man aged 46 years had F3 fibrosis on histological examination (Fig. 2b). His type IV collagen was 5.3 ng/mL, platelet 137×10^3 count/mm^3, TIMP-2 92 ng/mL and α-2-macroglobulin 255, and the regression function calculated his fibrosis score as 3.10.

Validation of discriminant function

Validation data of 69 patients (Table 3) were collected from the other six institutions in Japan. When applying

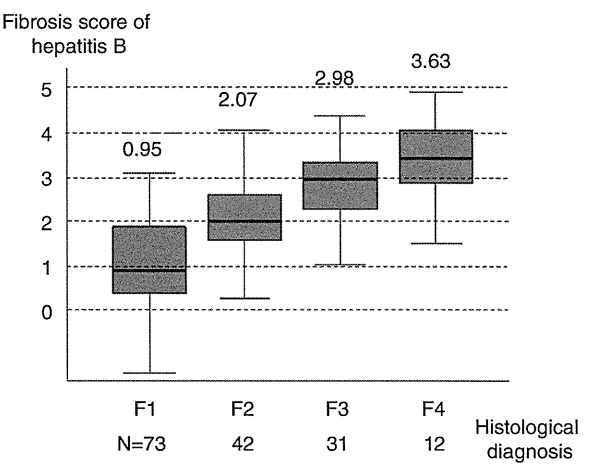

Figure 1 Box and whisker plots of fibrotic score of each histological fibrosis group in the training dataset. The fibrosis score of hepatitis B was generated by the function, $z = 1.40 \times ln$ (type IV collagen 7S) (ng/mL) − $0.017 \times$ (platelet count) (×1000^3/mm^3) + $1.24 \times ln$ (tissue inhibitor of matrix metalloproteinase-2) (ng/mL) + $1.19 \times ln$ (α-2-macroglobulin) (mg/dL) − 9.15.

Table 2 Correlation coefficients (Spearman's ρ) among fibrosis predictors used in multivariate analysis

	Platelet	gamma-globulin	*ln* (α-2-macroglobulin)	*ln* (hyaluronate)	*ln* (P-III-P)	*ln* (IV collagen)	*ln* (TIMP-2)
Platelet ($\times 10^3/mm^3$)	1.000	−0.214 ($P = 0.008$)	−0.260 ($P = 0.001$)	−0.384 ($P < 0.001$)	−0.045 ($P = 0.58$)	−0.297 ($P < 0.001$)	0.094 ($P = 0.24$)
γ-Globulin (g/dL)		1.000	0.276 ($P = 0.001$)	0.349 ($P < 0.001$)	0.342 ($P < 0.001$)	0.414 ($P < 0.001$)	0.268 ($P = 0.001$)
ln (α-2-macroglobulin) (mg/dL)			1.000	0.281 ($P < 0.001$)	0.141 ($P = 0.078$)	0.171 ($P = 0.032$)	−0.079 ($P = 0.32$)
ln (hyaluronic acid) (mg/L)				1.000	0.373 ($P < 0.001$)	0.493 ($P < 0.001$)	0.089 ($P = 0.27$)
ln (procollagen III peptide) (U/mL)					1.000	0.600 ($P < 0.001$)	0.145 ($P = 0.071$)
ln (type IV collagen) (mg/L)						1.000	0.358 ($P < 0.001$)
ln (TIMP-2) (mg/L)							1.000

TIMP, tissue inhibitor of matrix metalloproteinase.

the regression function for the validation set, the fibrosis score demonstrated good reproducibility, showing 1.33 in patients with chronic hepatitis of F1 ($n = 27$), 2.20 of F2 ($n = 20$), 3.11 of F3 ($n = 20$) and 5.30 of F4 ($n = 2$), respectively (Fig. 3). Although F4 fibrosis stage consisted of only two patients and the score 5.30 was regarded as of rather higher value, the scores of other stages of fibrosis were concordant with histological fibrosis.

Comparisons of efficacy with various fibrosis scores (Fig. 4)

In order to evaluate the efficacy and usefulness of the obtained FSB, we compared it with previously reported fibrosis scores using training data. AAR, APRI and FibroTest showed only slight correlation with actual histological stage. FIB-4 demonstrated an increasing trend of the score associated with histological fibrosis, but significant overlapping scores were found in F1–F4. Spearman's correlation coefficients of AAR, APRI, FIB-4 and FibroTest were 0.199 ($P = 0.012$), 0.265 ($P = 0.001$), 0.412 ($P < 0.001$) and 0.330 ($P < 0.001$), respectively. Our FSB showed a Spearman's correlation coefficient of 0.625 ($P < 0.001$), and was a much higher value than the others. The dichotomous discrimination function for cirrhosis and hepatitis C in Japanese patients[23] showed good differentiation also in patients with hepatitis B virus.

DISCUSSION

RECOGNITION OF SEVERITY of chronic hepatitis is essential in managing patients with chronic HBV infection: estimation of length of infection, existence of any previous hepatitis activity, presumption of current fibrotic stage, and prediction of future fibrosis progression and hepatocarcinogenesis. Differential diagnosis of cirrhosis from chronic hepatitis is especially important in the evaluation of chronic HBV infection. Identification of liver cirrhosis often leads to an important change in management of the patient: need for fiberscopic examination for esophageal varices, ultrasonographic exploration for the association of liver cancer, and prediction of hepatic decompensation. Guidelines published by the American Association of Study of Liver Disease[24] recommend liver biopsy for HBV carriers with aminotransferase elevation or for any candidates of antiviral therapy, because hepatic fibrosis sometimes shows unexpectedly far advancement to cirrhosis, and because it is very difficult to evaluate and translate the liver function tests or ultrasonographic findings compared to chronic hepatitis type C.

Table 3 Demography and laboratory data of 69 patients in training group

	F1 ($n = 27$)	F2 ($n = 20$)	F3 ($n = 20$)	F4 ($n = 2$)
Demographics				
Men : women	18:9	15:5	13:7	2:0
Age (median, range)	36 (13–64)	45 (14–64)	36.5 (24–59)	32 (25–39)
Laboratory data (median, range)				
WBC (×1000/mm^3)	5.0 (2.8–8.7)	5.8 (2.8–11.6)	5.3 (3.2–8.1)	3.85 (2.7–5.0)
Hemoglobin (g/dL)	14.8 (12.4–17.4)	15.0 (12.4–16.9)	14.4 (11.1–16.4)	14.4 (12.5–16.3)
Platelet (×1000/mm^3)	204 (86–322)	180 (90–275)	147 (90–276)	130 (67–183)
Albumin (g/dL)	4.4 (2.8–5.2)	4.2 (3.5–5.1)	4.3 (3.4–4.9)	4.45 (4.0–4.9)
Bilirubin (mg/dL)	0.9 (0.4–6.4)	0.8 (0.2–1.6)	0.75 (0.4–1.7)	1.15 (1.1–1.2)
AST (IU/L)	52 (17–575)	50.5 (21–272)	65 (22–284)	248.5 (51–446)
ALT (IU/L)	84 (16–1101)	101.5 (19–554)	86.5 (16–1113)	453.5 (74–833)
γ-GTP (IU/L)	42 (14–332)	54 (16–205)	52.5 (13–191)	193 (57–329)
γ-Globulin (g/dL)	1.30 (1.04–1.59)	1.35 (1.18–2.53)	1.62 (1.16–1.97)	1.545 (1.51–1.58)
γ-Globulin (%)	17.9 (14.3–22.1)	19.6 (15.5–30.8)	22.0 (16.5–24.6)	20.15 (19.3–21.0)
α-2-Macroglobulin (mg/dL)	287 (160–687)	270 (89–452)	272.5 (211–463)	389 (313–465)
Haptoglobin (mg/dL)	58 (<5–229)	74 (<5–154)	56.5 (<5–198)	<5 (<5–<5)
Apolipoprotein A-I (mg/dL)	146 (95–216)	137 (87–162)	120 (88–170)	100.5 (74–127)
Hyaluronic acid (μg/L)	27 (<5–113)	36 (10–1050)	59 (14–439)	331 (225–437)
TIMP-1 (ng/mL)	168.5 (83–302)	176 (127–408)	182 (104–303)	390.5 (283–498)
TIMP-2 (ng/mL)	76 (25–143)	86.5 (28–154)	77.5 (32–141)	100.5 (91–110)
Procollagen III peptide (U/mL)	0.71 (0.27–2.20)	0.88 (0.63–2.80)	0.995 (0.60–2.10)	1.75 (1.50–2.00)
Type IV collagen 7S (ng/ml)	3.6 (2.7–17.0)	5.25 (3.3–13.0)	5.7 (3.0–16.0)	15.5 (15.0–16.0)

ALT, alanine aminotransferase; AST, aspartate aminotransferase; γ-GTP, γ-glutamyl transpeptidase; TIMP, tissue inhibitor of matrix metalloproteinase; WBC, white blood cells.

Recently, non-invasive estimation of severity of liver fibrosis has been reported in patients with HBV-related chronic hepatitis.[2,6–13] However, these studies were principally aimed at differentiation of advanced fibrotic stages of F3 or F4 from mild fibrotic stages of F1 or F2. Those discrimination functions were insufficient to recognize the stepwise progression of viral hepatitis from F1–F4. This dichotomy (mild or severe) of chronic hepatitis B seemed less valuable in the study of disease progression, disease control abilities of antiviral drugs and estimation of histological improvement after anti-inflammatory drugs. A histology-oriented, practical and reliable formula is therefore required for the diagnosis and investigation of chronic hepatitis B.

This study aimed to establish non-invasive evaluation and calculation of liver fibrosis for patients with chronic hepatitis B virus infection. Although it was retrospectively performed as a multicenter study of eight institutions, judgment of histological diagnosis was independently performed by four pathologists in another hospital, who were informed only of the patient's age, sex and positive HBV infection. Objective judgment of the histological staging and grading in sufficient biopsy specimens could be obtained.

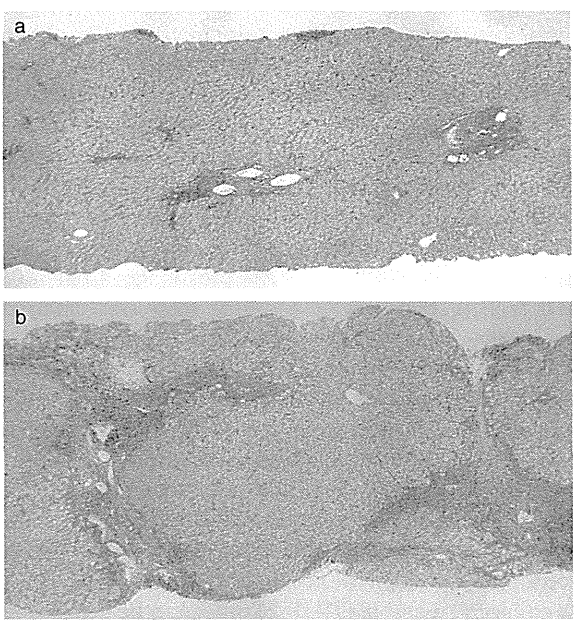

Figure 2 Case presentations of the training set. (a) A 28-year-old man with F1 fibrosis. Final regression function provided his fibrosis score as 0.99. (b) A 45-year-old man with F3 fibrosis. His regression coefficient was calculated as 3.10. Silver stain, ×40.

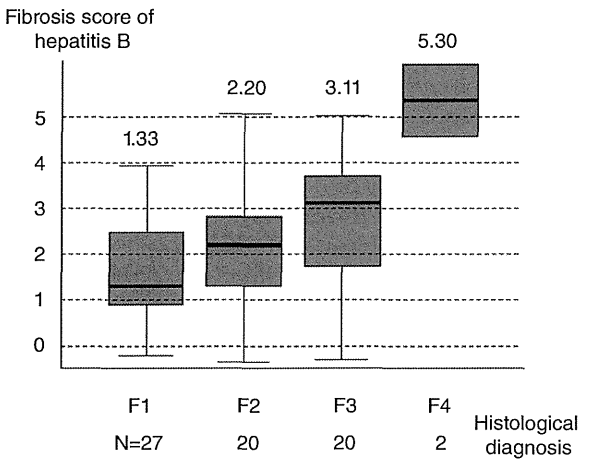

Figure 3 Box and whisker plots of fibrotic score of each group of histological fibrosis in the validation dataset. The fibrosis score of hepatitis B was generated by the function, $z = 1.40 \times ln$ (type IV collagen 7S) (ng/mL) $- 0.017 \times$ (platelet count) ($\times 1000^3/mm^3$) $+ 1.24 \times ln$ (tissue inhibitor of matrix metalloproteinase-2) (ng/mL) $+ 1.19 \times ln$ (α-2-macroglobulin) (mg/dL) $- 9.15$.

As many as 227 patients with chronic hepatitis B were analyzed in this study, who had been diagnosed as having chronic hepatitis or cirrhosis by liver biopsy performed in experienced liver units in Japan. To obtain the most suitable equation approximating histological fibrotic stage, multivariate analysis was performed using two demographic parameters (age and sex) and 21 hematological and biochemical markers with or without logarithmic transformation. They included many kinds of fibrosis markers: α-2-macroglobulin, haptoglobin concentration, haptoglobin typing, apolipoprotein A1, hyaluronic acid, TIMP-1, TIMP-2, procollagen III peptide and type IV collagen 7S Multiple regression analysis finally generated a first-degree polynomial function consisting of four variables: type IV collagen 7S, platelet count, TIMP-2 and α2-macroglobulin. A constant numeral (−9.15) was finally adjusted in the regression equation in order to obtain fitted figures for a fibrotic stage of F1–F4. From the magnitude of the standardized partial regression coefficient of individual variable in the function, platelet count demonstrated the most potent contribution toward the prediction of liver fibrosis. Type IV collagen 7S and *ln* (TIMP-2) proved to be the second and third distinctive power in the model, respectively.

The FSB was sufficiently fitted to actual fibrotic stages with certain overlapping as is usually found in histological ambiguity judged by pathologists. Because judgment of fibrosis in chronic hepatitis often shows a transitional histological staging, pathological examination cannot always make a clear-cut diagnosis discriminating F1–F4. Considering the limitation of the pathological difficulty in differentiating the four continuous disease entities, the obtained regression function showed satisfactory high accuracy rates in the prediction of liver disease severity. The FSB can provide one or two decimal places (e.g. 3.2 or 3.24) and the utility of the score is possibly higher than the mere histological stage of F1–F4. The reproducibility was confirmed by the remaining 67 patients' data obtained from the other six hospitals. Although the validation data were collected from a different geographic area and different chronological situation, the FSB showed similar results in prediction of histological staging.

The FSB seemed a very useful quantitative marker in evaluating fibrotic severity of hepatitis B patients without invasive procedures and without any specialized ultrasonography or magnetic resonance imaging. The FSB also has an advantage of measurement, in which old blood samples are available for retrospective assessment of varied clinical settings: for example, old sera from 20 years prior to the time of initial liver biopsy, or paired sera before and after long-term antiviral therapy. These kinds of retrospective assessments of fibrotic staging will be valuable in estimating a long-term progression of liver disease, in evaluating efficacy of long-term medication or other medical intervention, or in making a political judgment from the viewpoints of socioeconomic efficacy.

The score can be calculated for any patients with chronic HBV infection. Although this multiple regression model dealt with appropriate logarithmic transformation for non-normal distribution parameters, the regression analysis was based on a linear regression model. Very slight fibrosis can be calculated as less than 1.00, which is commonly found to a slight degree in chronic hepatitis with tiny fibrotic change as F0. Very severe fibrosis might be calculated as more than 4.00, which is an imaginary and nonsense number in the scoring system of fibrosis. The FSB is, however, very useful and valuable in a real clinical setting: estimation of severity of liver fibrosis in an outpatient clinic, evaluation of the natural progression of a patient's fibrosis over 10 years and assessment of a long-term administration of interferon in patients with chronic hepatitis B from the viewpoint of fibrotic change. Recent development of new nucleoside/nucleotide analogs requires evaluation for long-term histological advantage, for aggravation of hepatitis stage during viral and biochemical breakthrough caused by HBV mutation, and even for

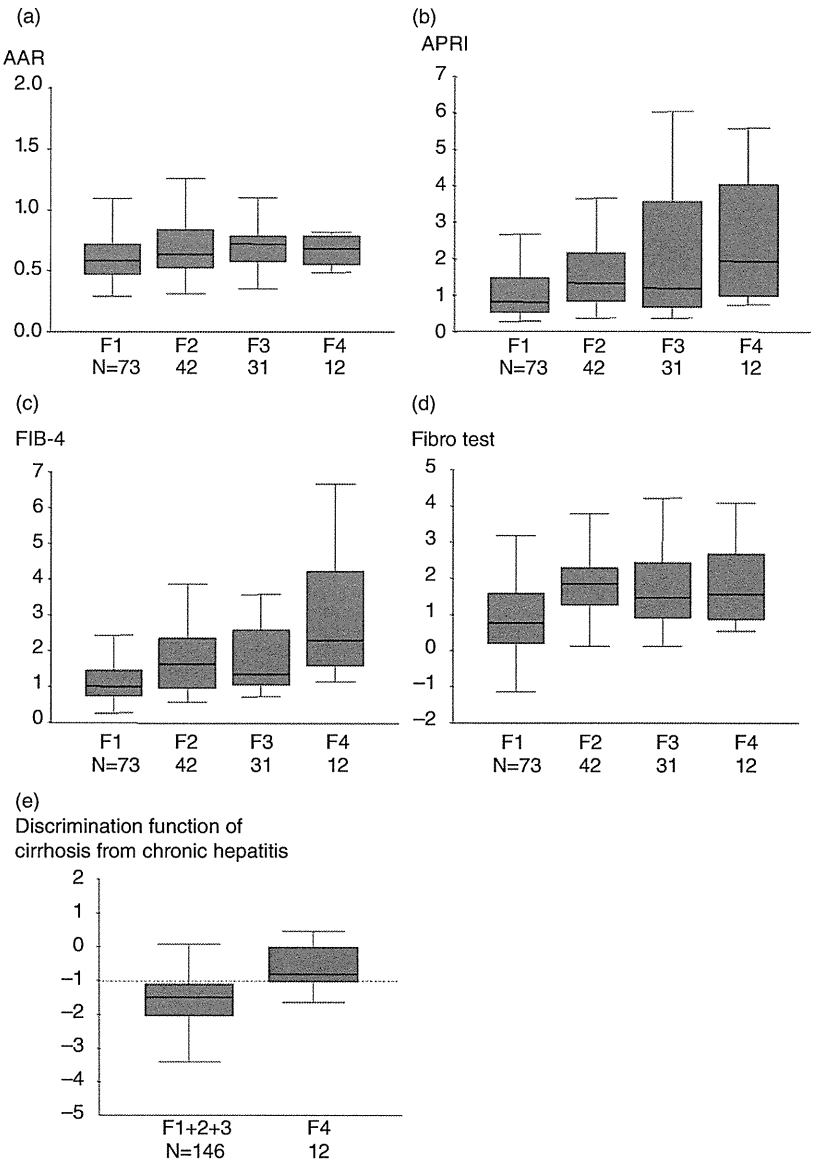

Figure 4 Previously published fibrosis scores. (a) Aspartate aminotransferase/alanine aminotransferase ratio (AAR),[19] (b) aspartate aminotransferase-to-platelet ratio index (APRI),[20] (c) FIB-4,[21] (d) FibroTest[22] and (e) discrimination function of cirrhosis from hepatitis in Japanese patients.[23]

the best management of patients with chronic hepatitis B. The FSB seems one of the ideal methods of approximating the fibrotic stage of chronic hepatitis B. Repeated measurement is quite suitable for patients with an unestablished treatment or trial, every 1 or 2 years, for example. Because the current regression function was generated from the data of HBV-related chronic liver disease, this equation would not be suitable for the recognition of hepatitis C virus-related chronic liver disease, alcoholic liver disease, and other congenital or autoimmune liver diseases. To recognize the latter diseases, other studies of individual diseases must be performed.

We compared the usefulness of the FSB with that of other fibrosis scores.[19–23] The more simple and less expensive AAR or APRI could not estimate fibrotic stages with poor correlation coefficients of 0.199 and 0.265, which are much lower than the coefficient of the FSB of 0.625. FibroTest, which contained three costly fibrosis markers (α-2-macroglobulin, haptoglobin and apolipo-

protein A1), also showed a low correlation coefficient of 0.330, suggesting that its usefulness was limited in HBV positive oriental patients. Although FIB-4 demonstrated the best coefficient of 0.412 among the fibrosis scores, significant overlaps were found between neighboring stages and obtained scores were not coordinated for real histological classification.

In conclusion, the FSB was a useful and reliable biomarker for prediction of liver fibrosis in patients with chronic HBV infection. The FSB is expected to be introduced and utilized in varied kinds of studies and trials. Its accuracy and reproducibility require further validation using higher numbers of patients in several countries other than Japan.

ACKNOWLEDGMENTS

THIS STUDY WAS proposed and initiated by Dr Shiro Iino and the project was performed with a grant from the Viral Hepatitis Research Foundation of Japan.

REFERENCES

1 Sandrin L, Fourquet B, Hasquenoph JM *et al.* Transient elastography: a new noninvasive method for assessment of hepatic fibrosis. *Ultrasound Med Biol* 2003; **29**: 1705–13.
2 Myers RP, Tainturier MH, Ratziu V *et al.* Prediction of liver histological lesions with biochemical markers in patients with chronic hepatitis B. *J Hepatol* 2003; **39**: 222–30.
3 Hanna RF, Kased N, Kwan SW *et al.* Double-contrast MRI for accurate staging of hepatocellular carcinoma in patients with cirrhosis. *AJR Am J Roentgenol* 2008; **190**: 47–57.
4 Hagiwara M, Rusinek H, Lee VS *et al.* Advanced liver fibrosis: diagnosis with 3D whole-liver perfusion MR imaging–initial experience. *Radiology* 2008; **246**: 926–34.
5 Taouli B, Chouli M, Martin AJ, Qayyum A, Coakley FV, Vilgrain V. Chronic hepatitis: role of diffusion-weighted imaging and diffusion tensor imaging for the diagnosis of liver fibrosis and inflammation. *J Magn Reson Imaging* 2008; **28**: 89–95.
6 Montazeri G, Estakhri A, Mohamadnejad M *et al.* Serum hyaluronate as a non-invasive marker of hepatic fibrosis and inflammation in HBeAg-negative chronic hepatitis B. *BMC Gastroenterol* 2005; **5**: 32.
7 Zeng MD, Lu LG, Mao YM *et al.* Prediction of significant fibrosis in HBeAg-positive patients with chronic hepatitis B by a noninvasive model. *Hepatology* 2005; **42**: 1437–45.
8 Chrysanthos NV, Papatheodoridis GV, Savvas S *et al.* Aspartate aminotransferase to platelet ratio index for fibrosis evaluation in chronic viral hepatitis. *Eur J Gastroenterol Hepatol* 2006; **18**: 389–96.
9 Kim BK, Kim Y, Park JY *et al.* Validation of FIB-4 and comparison with other simple noninvasive indices for predicting liver fibrosis and cirrhosis in hepatitis B virus-infected patients. *Liver Int* 2010; **30**: 546–53.
10 Wu SD, Wang JY, Li L. Staging of liver fibrosis in chronic hepatitis B patients with a composite predictive model: a comparative study. *World J Gastroenterol* 2010; **16**: 501–7.
11 Sökücü S, Gökçe S, Güllüoğlu M, Aydoğan A, Celtik C, Durmaz O. The role of the non-invasive serum marker FibroTest-ActiTest in the prediction of histological stage of fibrosis and activity in children with naïve chronic hepatitis B infection. *Scand J Infect Dis* 2010; **42**: 699–703.
12 Liu HB, Zhou JP, Zhang Y, Lv XH, Wang W. Prediction on liver fibrosis using different APRI thresholds when patient age is a categorical marker in patients with chronic hepatitis B. *Clin Chim Acta* 2011; **412**: 33–7.
13 Park SH, Kim CH, Kim DJ *et al.* Usefulness of Multiple Biomarkers for the Prediction of Significant Fibrosis in Chronic Hepatitis B. *J Clin Gastroenterol* 2011; **45**: 361–5.
14 Engstrom-Laurent A, Loof L, Nyberg A, Schroder T. Increased serum levels of hyaluronate in liver disease. *Hepatology* 1985; **5**: 638–42.
15 Murawaki Y, Ikuta Y, Koda M, Kawasaki H. Serum type III procollagen peptide, type IV collagen 7S domain, central triple-helix of type IV collagen and tissue inhibitor of metalloproteinases in patients with chronic viral liver disease: relationship to liver histology. *Hepatology* 1994; **20**: 780–7.
16 Fabris C, Falleti E, Federico E, Toniutto P, Pirisi M. A comparison of four serum markers of fibrosis in the diagnosis of cirrhosis. *Ann Clin Biochem* 1997; **34**: 151–5.
17 Desmet VJ, Gerber M, Hoofnagle JH, Manns M, Sheuer PJ. Classification of chronic hepatitis: diagnosis, grading, and staging. *Hepatology* 1994; **19**: 1513–20.
18 IBM SPSS Inc. *IBM SPSS for Windows Version 19.0 Manual.* Armonk NY, USA: SPSS Japan Inc., an IBM company, 2009.
19 Sheth SG, Flamm SL, Gordon FD *et al.* AST/ALT ratio predicts cirrhosis in patients with chronic hepatitis C virus infection. *Am J Gastroenterol* 1998; **93**: 44–8.
20 Wai CT, Greenson JK, Fontana RJ *et al.* A simple noninvasive index can predict both significant fibrosis and cirrhosis in patients with chronic hepatitis C. *Hepatology* 2003; **38**: 518–26.
21 Sterling RK, Lissen E, Clumeck N *et al.* Develoment of a simple noninvasive index to predict significant fibrosis in patients with HIV/HCV coinfection. *Hepatology* 2006; **43**: 1317–25.
22 Imbert-Bismut F, Ratziu V, Pieroni L *et al.* Biochemical imarkers of liver fibrosis in patients with hepatitis C virus infection: a prospective study. *Lancet* 2001; **357**: 1069–75.
23 Ikeda K, Saitoh S, Kobayashi M *et al.* Distinction between chronic hepatitis and liver cirrhosis in patients with hepatitis C virus infection. Practical Discriminant function using common laboratory data. *Hepatol Res* 2000; **18**: 252–66.
24 Lok ASF, McMahon BJ. AASLD Practice Guidelines. Chronic hepatitis B: update 2009. *Hepatology* 2009; **50**: 1–36.

EXPERIMENTAL CELL RESEARCH 319 (2013) 113–121

Available online at www.sciencedirect.com

SciVerse ScienceDirect

journal homepage: www.elsevier.com/locate/yexcr

Research Article

Leucine-rich repeat-containing G protein-coupled receptor 5 regulates epithelial cell phenotype and survival of hepatocellular carcinoma cells

Mariko Fukuma[a], *Keiji Tanese*[b], *Kathryn Effendi*[a], *Ken Yamazaki*[a], *Yohei Masugi*[a], *Mariko Suda*[a], *Michiie Sakamoto*[a,*]

[a]*Department of pathology, Keio University School of Medicine, Shinjuku-ku, Tokyo 160-8582, Japan*
[b]*Department of dermatology, Keio University School of Medicine, Shinjuku-ku, Tokyo 160–8582, Japan*

ARTICLE INFORMATION

Article Chronology:
Received 28 June 2012
Received in revised form
11 October 2012
Accepted 26 October 2012
Available online 2 November 2012

Keywords:
LGR5
GPR49
Hepatocellular carcinoma
Morphology
Motility

ABSTRACT

The leucine-rich repeat containing G protein-coupled receptor 5 (LGR5), also known as GPR49, is a seven-transmembrane receptor that is expressed in stem cells of the intestinal crypts and hair follicles of mice. LGR5 is overexpressed in some types of human cancer, and is one of the target genes of the Wnt signaling pathway. To explore the function of LGR5 in cancer cells, stable hepatocellular carcinoma (HCC) cell lines expressing FLAG-tagged LGR5 were established. Overexpression of LGR5 resulted in changes in cell shape from an extended flat (mesenchymal) phenotype to a round aggregated (stem cell-like) phenotype. Cells transfected with LGR5 showed higher colony forming activity, and were more resistant to a cytotoxic drug than cells transfected with empty vector. Overexpression of LGR5 inhibited cell motility. LGR5-transfected cells formed nodule type tumors in the livers of immunodeficient mice, whereas empty vector-transfected cells formed more invasive tumors. Down-regulation of LGR5 changed the morphology of HCC cells from the aggregated phenotype to an extended spindle phenotype, and cell motility was increased. This is the first study reporting the functional role of LGR5 in the biology of HCC cells, and the results suggest that aberrant expression of LGR5 regulates epithelial cell phenotype and survival.

Introduction

The leucine-rich repeat-containing G protein-coupled receptor 5 (LGR5), aliases G protein-coupled receptor 49 (GPR49), FEX, GPR67, GRP49, HG38, MGC117008, is structurally related to members of the glycoprotein hormone receptor family. In mice, deficiency of this gene causes neonatal lethality as a result of ankyloglossia [1]. LGR5 deficiency also induces premature differentiation of Paneth cells [2]. Recent studies from the Netherlands showed that in a mouse model, the homolog of this gene was a marker of intestinal and hair follicle stem cells. Introduction of an adenomatous polyposis coli (APC) mutation into LGR5-expressing cells increased the incidence of adenomas in mouse intestinal epithelial cells [3–5].

*Correspondence to: Department of pathology, Keio University School of Medicine, 35 Shinanomachi, Shinjuku-ku, Tokyo 160-8582, Japan. Fax: +81 3 3353 3290.
E-mail address: msakamot@z5.keio.jp (M. Sakamoto).

0014-4827/$ - see front matter © 2012 Elsevier Inc. All rights reserved.
http://dx.doi.org/10.1016/j.yexcr.2012.10.011